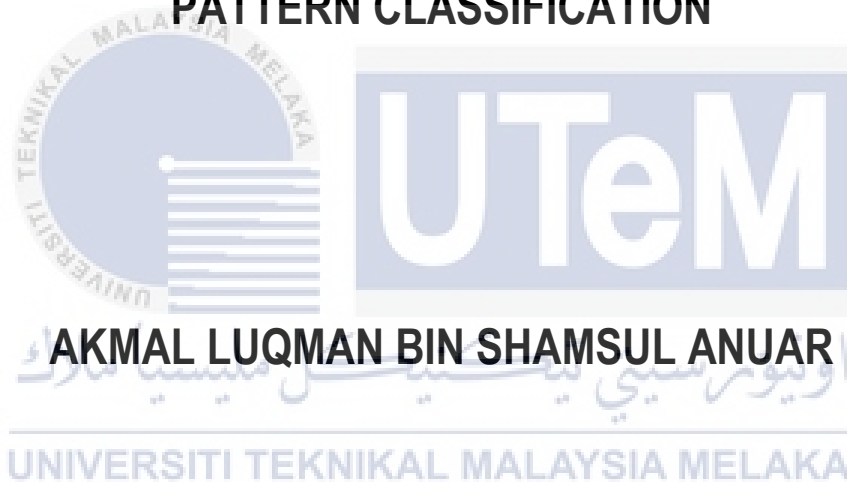




MULTIMODAL DEEP LEARNING OF POSTURE AND GAIT PATTERN CLASSIFICATION



BACHELOR OF ELECTRICAL ENGINEERING WITH HONOURS

2024



Faculty of Electrical Technology and Engineering



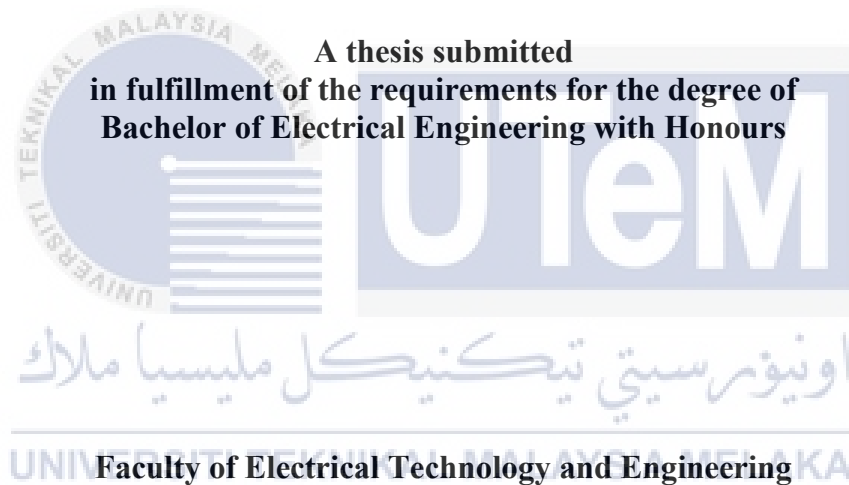
Akmal Luqman Bin Shamsul Anuar

Bachelor of Electrical Engineering with Honours

2024

**MULTIMODAL DEEP LEARNING OF POSTURE AND GAIT PATTERN
CLASSIFICATION**

AKMAL LUQMAN BIN SHAMSUL ANUAR



UNIVERSITI TEKNIKAL MALAYSIA MELAKA

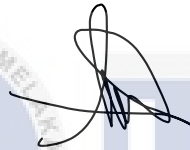
2024

DECLARATION

I declare that this thesis entitled “ MULTIMODAL DEEP LEARNING OF POSTURE AND GAIT PATTERN ” is the result of my own research except as cited in the references. The thesis has not been accepted for any degree and is not concurrently submitted in candidature of any other degree.

Signature

:



Name

:

AKMAL LUQMAN BIN SHAMSUL ANUAR

Date

:

21/6/2024

اونيورسيتي تيكنيكل مليسيا ملاك
UNIVERSITI TEKNIKAL MALAYSIA MELAKA

APPROVAL

I hereby declare that I have checked this thesis and in my opinion, this thesis is adequate in terms of scope and quality for the award of the Bachelor of Electrical Engineering with Honours.

Signature :



Supervisor Name

DR. EZREEN FARINA BINTI SHAIR

Date

21/6/2024



DEDICATION

To my beloved family.

Thank you for always pushing me forward. I will always pursue for happiness.



ABSTRACT

An individual's gait is a unique characteristic impacted by various variables. Gait patterns, the way a person walks, can be used for verification as they are often unconscious behaviors. Conventional gait pattern studies use machine learning, which requires complex data extraction and achieves limited accuracy with unimodal data. This study employs deep learning to classify gait patterns into walking straight, turning right, and turning left. It also explores the impact of unimodal versus multimodal data for higher accuracy. Advanced algorithms are used to visualize 2- and 3-dimensional gait and posture data in Python, processing the data for deep learning. Gait patterns from 14 participants on different paths along a corridor are extracted. The methodology is divided into three phases: data pre-processing, data processing, and data classification. In data pre-processing, Spyder software is used to visualize each participant's gait and posture frames based on timestamp files from an open-source database. In data processing, the Time Frequency Domain (TFD) method, utilizing Short Time Frequency Transformation (STFT) in Spyder, is chosen to overcome limitations in frequency and time domains. In data classification, results from unimodal and multimodal data using deep learning algorithms, specifically Convolutional Neural Network (CNN) and Recurrent Neural Network (RNN), are compared for different gait situations.

ABSTRAK

Gaya berjalan seseorang individu adalah ciri unik yang dipengaruhi oleh pelbagai pembolehubah. Corak gaya berjalan, cara seseorang berjalan, boleh digunakan untuk pengesanan kerana ia selalunya merupakan tingkah laku tidak sedarkan diri. Kajian corak gait konvensional menggunakan pembelajaran mesin, yang memerlukan pengekstrakan data yang kompleks dan mencapai ketepatan terhadap data unimodal. Kajian ini menggunakan pembelajaran mendalam untuk mengklasifikasikan corak berjalan kepada berjalan lurus, membelok ke kanan dan membelok ke kiri. Ia juga meneroka kesan data unimodal berbanding multimodal untuk ketepatan yang lebih tinggi. Algoritma lanjutan digunakan untuk menggambarkan data gait dan postur 2 dan 3 dimensi dalam Python, memproses data untuk pembelajaran mendalam. Corak berjalan daripada 14 peserta di laluan berbeza di sepanjang koridor diekstrak. Metodologi dibahagikan kepada tiga fasa: pra-pemprosesan data, pemprosesan data, dan klasifikasi data. Dalam pra-pemprosesan data, perisian Spyder digunakan untuk menggambarkan bingkai gaya berjalan dan postur setiap peserta berdasarkan fail cap masa daripada pangkalan data sumber terbuka. Dalam pemprosesan data, kaedah Domain Frekuensi Masa (TFD), menggunakan Transformasi Frekuensi Masa Singkat (STFT) dalam Spyder, dipilih untuk mengatasi had dalam domain kekerapan dan masa. Dalam klasifikasi data, hasil daripada data unimodal dan multimodal menggunakan algoritma pembelajaran mendalam, khususnya Rangkaian Neural Konvolusi (CNN) dan Rangkaian Neural Berulang (RNN), dibandingkan untuk situasi berjalan yang berbeza.

ACKNOWLEDGEMENTS

A massive appreciation I would like to express to my supervisor, Dr. Ezreen Farina Binti Shair for her guidance and inputs that helped me to finish my final year project. I am grateful for all her tolerance and support.

My sincere appreciation also goes to all my friends that went through ups and downs with me. Their views on everything are directly and indirectly helped me to finish my final year project.

Lastly, I want to thank me.



TABLE OF CONTENTS

| | PAGE |
|---|------------|
| DECLARATION | |
| APPROVAL | |
| DEDICATION | |
| ABSTRACT | i |
| ABSTRAK | ii |
| ACKNOWLEDGEMENTS | iii |
| TABLE OF CONTENTS | iv |
| LIST OF TABLES | vi |
| LIST OF FIGURES | vii |
| LIST OF SYMBOLS AND ABBREVIATIONS | ix |
| LIST OF APPENDICES | x |
| CHAPTER 1 INTRODUCTION | 11 |
| 1.1 Research Background | 11 |
| 1.2 Motivation | 12 |
| 1.3 Problem Statement | 13 |
| 1.4 Research Objective | 14 |
| 1.5 Scope of Research | 14 |
| CHAPTER 2 LITERATURE REVIEW | 16 |
| 2.1 Introduction | 16 |
| 2.2 Needs to Study on Gait Pattern Classification | 16 |
| 2.3 Gait Pattern and Phases | 20 |
| 2.4 Gait Parameters | 23 |
| 2.5 Inertial Measurement Unit (IMU) | 25 |
| 2.5.1 Xsens MTw Awinda | 25 |
| 2.6 Comparison Between Deep Learning and Machine Learning | 27 |
| 2.6.1 Convolutional Neural Network (CNN) | 30 |
| 2.6.2 Recurrent Neural Network (RNN) | 31 |
| 2.7 Comparison Between Unimodal and Multimodal | 34 |
| CHAPTER 3 METHODOLOGY | 35 |
| 3.1 Introduction | 35 |
| 3.2 Dataset Description | 37 |
| 3.3 Data Collection Scenarios | 37 |

| | | |
|-------------------|--|-----------|
| 3.4 | Ethics and Safety of Data Collection Scenarios | 39 |
| 3.5 | Data Pre-processing | 39 |
| 3.6 | Data Processing | 43 |
| 3.7 | Data Classification | 47 |
| 3.8 | Summary | 51 |
| CHAPTER 4 | RESULTS AND DISCUSSION | 52 |
| 4.1 | Introduction | 52 |
| 4.2 | Data Pre-Processing | 52 |
| 4.3 | Data Processing | 54 |
| 4.4 | Data Classification | 57 |
| CHAPTER 5 | CONCLUSION AND RECOMMENDATIONS | 61 |
| 5.1 | Conclusion | 61 |
| 5.2 | Future Works | 62 |
| REFERENCES | | 63 |
| APPENDICES | | 68 |



LIST OF TABLES

| TABLE | TITLE | PAGE |
|-----------|---|------|
| Table 2-1 | Past Studies for diseases related to gait abnormalities | 17 |
| Table 2-2 | Gait characteristics of diseases that are related to gait abnormalities | 18 |
| Table 2-3 | Past studies related with gait pattern classification using machine learning and deep learning. | 27 |
| Table 2-4 | Comparison between unimodal and multimodal data | 34 |
| Table 3-1 | Gait and posture depth data for participant 1 aligned with time | 44 |
| Table 4-1 | Comparison between CNN and RNN also multimodal and unimodal data | 60 |



LIST OF FIGURES

| FIGURE | TITLE | PAGE |
|---------------|---|-------------|
| Figure 2-1 | Normal human gait phases | 22 |
| Figure 2-2 | Visualization of gait parameters | 24 |
| Figure 2-3 | MTW Motion Tracker | 26 |
| Figure 2-4 | Awinda Dongle | 26 |
| Figure 2-5 | CNN layer | 31 |
| Figure 2-6 | RNN Structure | 32 |
| Figure 2-7 | Motion prediction using RNN | 33 |
| Figure 2-8 | Enhanced RNN structure for motion prediction | 33 |
| Figure 3-1 | Overview of methodology | 36 |
| Figure 3-2 | Gait and posture data collection setup for participants | 38 |
| Figure 3-3 | Overview flowchart of data-preprocessing coding | 40 |
| Figure 3-4 | Overview flowchart of data processing coding | 45 |
| Figure 3-5 | Overview flowchart of data classification coding | 48 |
| Figure 4-1 | Participants' posture data visualization while walking | 53 |
| Figure 4-2 | Participants' gait data visualization while walking | 53 |
| Figure 4-3 | TFR diagram for participant 1 turning left | 54 |
| Figure 4-4 | TFR diagram of participant 1 turning right | 55 |
| Figure 4-5 | TFR diagram of participant 1 walking straight | 55 |
| Figure 4-6 | CNN Multimodal Classification Accuracy Percentage | 57 |
| Figure 4-7 | RNN Multimodal Classification Accuracy Percentage | 57 |
| Figure 4-8 | CNN Unimodal Classification Accuracy Percentage | 58 |



LIST OF SYMBOLS AND ABBREVIATIONS

| | | |
|---------|---|--------------------------------------|
| TFR | - | Time Frequency Representation |
| STFT | - | Short Time Fourier Transformation |
| OA | - | Osteoarthritis |
| ECG | - | Electrocardiogram |
| TFD | - | Time Frequency Diagram |
| CNN | - | Convolutional Neural Network |
| RNN | - | Recurrent Neural Network |
| FOG | - | Freezing of Gait |
| HS | - | Heel Strike |
| TO | - | Toe Off |
| AI | - | Artificial Intelligence |
| SVM | - | Support Vector Machine |
| sEMG | - | Surface Electromyographic |
| DCNN | - | Deep Convolutional Neural Network |
| Bi-LSTM | - | Bidirectional long short-term memory |
| IMU | - | Inertial Measurement Unit |

UNIVERSITI TEKNIKAL MALAYSIA MELAKA

LIST OF APPENDICES

| APPENDIX | TITLE | PAGE |
|------------|-----------------------|------|
| APPENDIX A | TFR OF PARTICIPANTS | 68 |
| APPENDIX B | PARTICIPANTS METADATA | 81 |



CHAPTER 1

INTRODUCTION

1.1 Research Background

In today's gait pattern analysis studies, radiology and medical evaluation such as X-ray are used. Although an X-ray scanner can diagnose knee osteoarthritis (OA) with great precision, these advantages come with a cost. Additionally, it is not recommended for patients to be often exposed to X-rays during medical evaluations, which makes it challenging to track the development of knee OA over time [1]. This is where deep learning can take place. Deep learning will overcome these challenges such as patients will not have to be exposed to radiology for a long period of time and it will also decrease the cost for gait pattern evaluation. Furthermore, deep learning method can help to improve the accuracy rate of gait pattern analysis.

This deep learning method will work with multimodal datasets. Current studies that use unimodal system exhibits numerous shortcomings such as noisy information, intra-class variation and inter-class resemblance [2]. By using multimodal datasets, noisy information can be extinguished. Based on the studies that have been conducted, the multiple device identification found in current smartwatches provides a convenient substitute for the standard smartphone methods of authentication [2]. Its main benefit is that identification can be done without requiring input from the user. The user's gait may be determined from the paces at which he walks, which is determined by the smartphone's inbuilt sensors, and his cardiac activity can be deduced from the electrocardiogram (ECG)

that the watch records [2]. It is simple to merge those patterns and utilize them for authentication.

The integration of multimodal datasets and deep learning method prove to be beneficial for patients and also medical practitioners. This work shows the enormous potential for diagnostics and treatment components to transfer from clinical settings to the home, decreasing costs and the strain on both practitioners and patients. This is especially important given the ageing population's growing need for medical support [3]. Furthermore, it can help medical professionals to identify which gait cycle that the patient struggles the most and allow the professionals to focus more on that specific gait cycle to help the patient [4].

1.2 Motivation

Nowadays, there are many different studies that has been conducted regarding diseases that are related to gait abnormalities. Some of the studied diseases are Alzheimer [5], Freezing of Gait which is a symptom of Parkinson's Disease [6] and Multiple Sclerosis [7]. A few statistics for Alzheimer, Parkinson and Multiple Sclerosis were found. Globally, roughly 50 million individuals suffer from dementia and Alzheimer's disease. It has been shown that there is a close relationship between dementia, ageing, and abnormal gait [8]. For Parkinson disease, it affects approximately 1% of people over 60, and the frequency rises with age. Parkinsonism is an illness that affects about 20% of adults over the age of 80. It is characterized by tremor, bradykinesia, rigidity, and instability of posture in different configurations that leads to gait abnormalities [9]. While for Multiple Sclerosis disease, in 93.7 percent of cases of multiple sclerosis, there is a loss in gait efficiency. Throughout any twelve-month period, the majority of persons (63%) who have multiple sclerosis will experience a fall and 45% of those people will go on to have falls on a

regular basis [10]. Based on past studies, it is found that each of the diseases has its own gait abnormalities characteristics. For Alzheimer, the patient exhibits lack of balance in their steps [5]. For Freezing of Gait, the patient exhibit reduced leg movement speed and steps shorter but faster [6]. Lastly, for Multiple Sclerosis, the patient exhibit longer stride duration, slower gait, larger base of support and shorter single support period in their steps [7].

By conducting this study that analyzing gait and posture pattern by using deep learning with multimodal data, it is hope that this study can lead to future study that can detect the early stage of the gait pattern related diseases by inspecting and analyzing the gait and posture pattern.

1.3 Problem Statement

Healthcare, assistive technology, and human-computer interaction are just a few of the fields that depend on the understanding and classification of human posture and gait patterns. Classifying complicated and variable posture and gait patterns remains an enormous challenge, particularly in everyday life, unregulated contexts, even if artificial intelligence has showed promise in picture and sensor data processing.

In current method for example machine learning, it requires long and intricate procedure in extracting the data manually. The rate of accuracy of this machine learning method also hugely depends on this data extracting. Existing methods also fail to attain high accuracy and generalization because it frequently rely on single-modal data sources. On the other hand, processing data with Time Domain method require a lot of processing and frequent sampling for some condition [11] while for Frequency domain, there is only little intricacy in signal analysis involved which means it can only process straight forward and simple signal and data and could not work with complex data [12]. Consequently, the

issue at hand is the requirement for a method with analyzing data with Time Frequency Domain, multimodal data and efficient deep learning system for the classification of posture and gait.

1.4 Research Objective

The main aim of this research is to classify gait pattern and posture based on the specific dataset with reasonable accuracy. Specifically, the objectives are as follows:

- a) To analyze accelerometer & camera data during walking using Time Frequency Domain.
- b) To classify gait and posture pattern using multimodal deep learning.
- c) To compare unimodal & multimodal deep learning result based on its accuracy.

1.5 Scope of Research

The simulation of physiological data that were used to evaluate the gait pattern is the main goal of this study. Modern techniques must be used to construct the physiological signals, and the process must be followed progressively. Dataset that were used was collected and taken using camera and accelerometer by Manuel Palermo and published in an open-source site, Physionet. The time-frequency domain (TFD) technique is used to extract the properties of physiological data in order to obtain a STFT graph of three distinct walking situations: walking straight ahead, walking right on a corridor, and walking left on a corridor. The best classifier to use for physiological signal applications utilizing CNN and RNN networks will also be determined as part of this study. Software called Spyder was used to visualize the excel file data that contains gait and posture data of the

participants and were also used to generate the STFT graphs before feeding the graphs to the deep learning classifier.



CHAPTER 2

LITERATURE REVIEW

2.1 Introduction

This chapter starts with the diseases that are related to gait pattern abnormalities to explain on the needs for study regarding gait pattern classification, explanation about gait pattern and its phases, deep learning classifiers and comparison to machine learning and also comparison between multimodal and unimodal dataset. Next, a discussion of the best method for action or suggestion will follow, along with a description of the literature review.

2.2 Needs to Study on Gait Pattern Classification

A methodical evaluation of the variables that define how people walk is called gait analysis. It is widely employed in many different contexts in particular, clinical studies of abnormal gait associated with cognitive deficits, non-neurological injuries, and neurological impairments that grow into other kinds of functional problems [13]. This study can help to find abnormal gait pattern that can lead to discovering diseases related to the abnormal gait pattern. There are several past studies that have been conducted regarding abnormalities in gait pattern. Table 2-1 shows past studies that have been conducted for diseases related to gait abnormalities.

Table 2-1 Past Studies for diseases related to gait abnormalities

| Title | Gait Abnormalities |
|---|--|
| Deep Learning based Gait Abnormality Detection using Wearable Sensor System [13] | <ul style="list-style-type: none"> • Hemiplegic • Parkinsonian • Sensory-Ataxic |
| Prediction of Freezing of Gait in Parkinson's Disease Using Wearables and Machine Learning [6] | <ul style="list-style-type: none"> • Freezing of Gait (FOG) (A symptom of Parkinson's disease) |
| Application of Supervised Machine Learning Algorithms in the Classification of Sagittal Gait Patterns of Cerebral Palsy Children with Spastic Diplegia [14] | <ul style="list-style-type: none"> • Categorization of Cerebral Palsy children's sagittal gait patterns with spastic diplegia |
| Early Alzheimer's Disease Diagnosis Using Wearable Sensors and Multilevel Gait Assessment: A Machine Learning Ensemble Approach [5] | <ul style="list-style-type: none"> • Early Diagnosis of Alzheimer's Disease |
| Deep Learning for Multiple Sclerosis Differentiation Using Multi-Stride Dynamics in Gait [7] | <ul style="list-style-type: none"> • Multiple Sclerosis |

These are the past studies that were found regarding diseases that exhibit abnormalities in the patients' gait pattern.

From past studies, each disease related to gait pattern abnormalities have its own gait characteristics. Table 2-2 shows the finding from past studies about gait characteristics that patient with gait abnormalities diseases exhibit.

Table 2-2 Gait characteristics of diseases that are related to gait abnormalities

| Disease | Gait Characteristics |
|---|---|
| Parkinson | <ul style="list-style-type: none"> • Trunk and pelvis rotate simultaneously. (For normal gait, trunk rotation is followed by pelvic rotation.) • Less step length • Tremor while walking |
| Hemiplegic | <ul style="list-style-type: none"> • The afflicted leg frequently exhibits plantar flexion and extension. • Leg circumduction is frequently observed during the swing phase. • Stance with the ipsilateral arm flexed. |
| Sensory Ataxic | <ul style="list-style-type: none"> • Lack of awareness of joint and limb position that leads to stomping. • Not able of sensing where their foot is in relation to the floor leads to asymmetrical gait. • Less step length • Wide based stance |
| Freezing of Gait (Parkinson's symptom) | <ul style="list-style-type: none"> • Reduced leg movement speed • Steps shorten and get faster. |
| Alzheimer | <ul style="list-style-type: none"> • Lack of balance |
| Multiple Sclerosis | <ul style="list-style-type: none"> • Longer stride duration. • Slower gait • Larger base of support • Shorter single support period |

Study of gait proved to be beneficial and abnormal gait patterns were found based on past studies conducted. To further understand the gait classification, normal gait pattern and phases needs to be understood.



2.3 Gait Pattern and Phases

Every normal human have gait phases that are almost the same from one's perspective. [15] stated that a common gait cycle are comprised of eight phases, beginning with the first foot impact and ending with the terminal swing, or the subsequent foot impact. These eight phases can be divided into two primary periods, stance cycle [16] and swing cycle [15]. To further understand this stance cycle and swing cycle, [17] explained that the stance cycle involves the duration during which a person's foot touches the ground from any angle. On the other hand, the swing cycle begins as soon as the stance cycle is over and is characterized by a forward-facing instant of leg swing. To further break down these phases, according to [17], a stance time can be further divided into five distinct parts:

- Heel Strike: The heel is making contact with the floor.
- Foot Flat: This position involves total contact between the foot and the floor.
- Mid-Stance: This is merely the middle part of the stride.
- Heel Off: This refers to the act of the heel lifting off the floor.
- Toe Off: This refers to the act of the toe leaving the floor.

While for swing cycle, the phases are divided into three distinct parts:

- Acceleration: The attempt is made to move the leg forward.
- Mid-Swing: This part of the swing involves keeping a leg in the center of the swing phase.
- De-acceleration: Attempting to slow down the leg for the subsequent heel, one becomes ready for the subsequent stance phase.

The stance cycle makes up 60% of the gait cycle on average, whereas the swing cycle makes up 40%. Additionally, each phase contains a series of both Single Support and Double Support, when only one foot is in contact with the ground during each sub-cycle [18].

In other finding by [16] states that gait cycle includes:

- First contact: also known as heel strike (HS), this is the instant the foot makes contact with the ground.
- Loading response: this stage starts as soon as the foot makes contact with the ground and lasts until the opposite leg is raised for the swing phase.
- Midstance: the moment that begins when the opposite leg is raised off the ground and ends when the body weight is in line with the forefoot.
- Terminal stance: this phase lasts from the moment the heel rises in the frontal plane until the opposite leg makes first contact.
- Pre-swing: this stage begins with the opposite leg's first contact and concludes with the same leg being raised off the ground.
- Swing stage: First swing: this stage, also known as toe off (TO), involves raising the foot off the ground and continuing until the knee flexion reaches its maximum range.
- Mid swing: this stage lasts until the tibia is vertical and starts right after bending the knee.
- Terminal swing: this stage starts just prior to the first point of contact and continues after the tibia is vertical.

For stance cycle, the stages involved are first contact, loading response, mid stance, terminal stance, and pre-swing while for swing cycle, the stages involved are first swing, mid swing and terminal swing. To further understand about gait phases, Figure 2-1 shows the visualization of human walking through each gait phase.

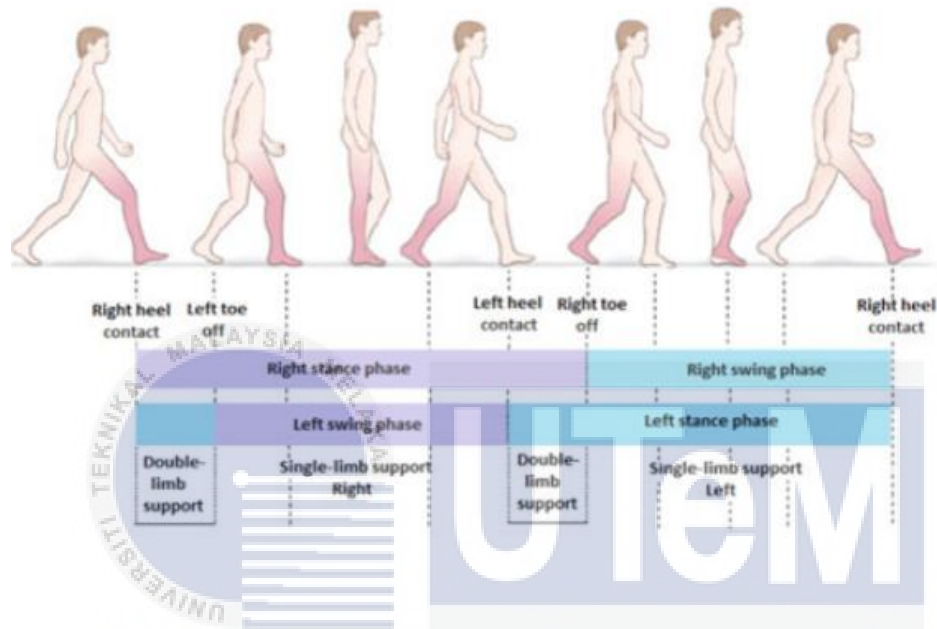


Figure 2-1 Normal human gait phases

To compare, both of the findings are very much identical to each other. Both of the findings involved stance and swing cycle. Using these gait cycle, gait analysis to analyze human gait can be done because human gait is a fundamental function, and a person's everyday stride patterns reveal important details about their psychological and physical well-being [19]. Other than psychological, physical well-being and gait related diseases, gait also can be used to determine a person's age, sex and diagnosis of illnesses [17]. To do this gait analysis, we need to determine gait parameters to distinguish every gait pattern according to its classification.

2.4 Gait Parameters

The following is a list of the most popular statistical parameters that might be derived from the detection of gait cycle [20]:

- Step length (m) is the measurement of the separation between one foot (Heel Strike) and the opposing feet at the beginning of contact.
- Stride length (m) is the space between consecutive locations of first contact (Heel Strike) made by the same foot.
- Step width (m) is the distance measured laterally between each foot.
- Step time (s) is the interval between both heel strikes in a row.
- Gait Cycle Time or Stride Time (s) is the total amount of time required to finish a gait cycle and the interval separating two successive heel strikes by the exact same foot.
- Gait Speed (m/s) is the stride length split by the total amount of gait cycle time.
- Cadence (steps/min) is the total amount of steps in a minute (steps/min).

UNIVERSITI TEKNIKAL MALAYSIA MELAKA

Figure 2-2 shows the visualization of gait parameters. As explained above, it can be seen that step length is indeed the measurement of separation between one foot and the other foot at the start contact while stride length is the measurement of separation at the start contact made by the same foot. On the other hand, step width is the measurement of distance laterally between each foot. By knowing all these parameters, it can help to classify gait patterns efficiently.

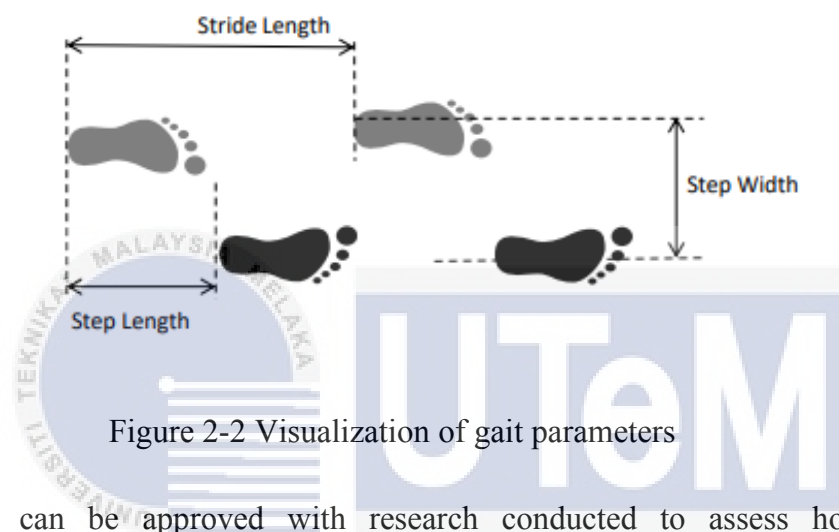


Figure 2-2 Visualization of gait parameters

This can be approved with research conducted to assess how an 8-week hippocampal treatment intervention affects walking ability and spatiotemporal gait characteristics in relapsing-remitting multiple sclerosis patients [21]. In order to conduct the research, spatiotemporal gait parameters were taken and analyzed and the parameters that were taken were gait speed (m/s), cadence (steps/min), step length (m), step width (m), stance time (s) and step time (s). After analyzing the gait parameters, it is found that 8-week hippocampal treatment intervention does bring impact by improving walking ability and spatiotemporal gait characteristics in relapsing-remitting multiple sclerosis patients [21].

After understanding gait parameters, gait and posture data can be collected and measured using an electronic device that integrates multiple sensors known as Inertial

Measurement Unit (IMU). These sensors reading data is a crucial part before feeding the data into the artificial intelligence (AI) technology like deep learning for further analysis.

2.5 Inertial Measurement Unit (IMU)

An electrical device that combines several sensors, including accelerometers, gyroscopes, and magnetometers, is called an Inertial Measurement Unit. This electronic gadget could have a secure digital (SD) card, an antenna (wireless technology), or even an output pin that is connected via wire to a base station. The most widely used abbreviation for this electronic gadget is (IMU) [22]. A major innovation in the field of biomechanics and wearable sensors was the development of the inertial measurement unit (IMU), which allows for spatiotemporal and kinematic assessments. These devices are affordable, enable the evaluation of nearly infinite steps, and enable the evaluation of gait and movement disorders outside of the restricted settings of clinical and research laboratories [23]. One of the examples for Inertial Measurement Unit is Xsens MTw Awinda.

2.5.1 Xsens MTw Awinda

Xsens' second generation wireless inertial-magnetic movement sensor is called the MTw Awinda. The MTw provides extremely precise orientation through a hidden setup, enabling real-time 3D kinematic applications with many motion trackers [24]. Figure 2-3 and Figure 2-4 shows the The Xsens MTw Awinda hardware.



Figure 2-3 MTW Motion Tracker



Figure 2-4 Awinda Dongle

Figure 2-3 shows the MTW Motion Tracker. The motion tracker weighs 16g and measures 47mm by 30mm by 13mm in its packaging. The MTw motion tracker uses inertial sensor components, specifically a 3D accelerometer and a 3D rate gyroscope, to detect motion. It also has a thermometer, a barometer, and a 3D magnetometer [24].

Figure 2-4 shows the Awinda Dongle. The Awinda Dongle is a compact USB gadget that measures just 45 mm by 20.4 mm by 10.6 mm when it has a USB connector and 33 mm by 20.4 mm by 10.6 mm when it does not [24].

After the gait and posture data is collected using Inertial Measurement Unit (IMU), then the data will be feed into Artificial Intelligence algorithms.

2.6 Comparison Between Deep Learning and Machine Learning

Table 2-3 shows past studies that have been conducted and its findings about gait patterns classification using machine learning and deep learning. Table 2-3 also contains type of sensors that were used to conduct each study, type of gait pattern classification, type of machine learning and deep learning algorithms that were used and the accuracy result of the algorithms to classify the gait pattern.

Table 2-3 Past studies related with gait pattern classification using machine learning and deep learning.

| Author | Type of Sensor | Gait Type of Classification | Classification Algorithm | Result |
|---|------------------|-----------------------------|--|-----------------------|
| Using Machine Learning Algorithms for Identifying Gait Parameters Suitable to Evaluate Subtle Changes in Gait in People with Multiple Sclerosis[25] | - Accelerometers | - Healthy | - Decision Tree | - Decision Tree = 62% |
| | - Gyroscopes | - Mild disability | - KNN | - KNN = 61.3% |
| | - Magnetometers | - Experienced fatigue | - SVM (Linear Kernel) Machine Learning | - SVM = 63.2% |

| | | | | |
|--|--|--|--|---|
| Supervised machine learning scheme for electromyography-based pre-fall detection system[26] | - Sema Sensor | - Human imbalance detection | - Surface Electromyographic (sEMG)-based Machine Learning | - The solution based on sEMG reaches 89.5% sensitivity and 91.3% specificity. |
| A Deep Learning Approach to EMG-Based Classification of Gait Phases during Level Ground Walking [27] | - Stance/swing phases - Prediction of the foot-floor-contact signal | - Natural deceleration, reversing, curve, and acceleration | - Surface Electromyographic (sEMG)-based Machine Learning | - Results, indeed, showed an average classification accuracy of 94.9 for learned subjects and 93.4 for unlearned ones |
| Deep Learning-Based Multimodal Abnormal Gait Classification Using a 3D Skeleton and Plantar Foot Pressure [28] | - Depth Camera - Plantar Foot Pressure | - Normal Gait - Abnormal Gait Eg: (antalgic, lurching, steppage, stiff-legged, and Trendelenburg) | - Recurrent Neural Network (RNN) - Convolutional Neural Network (CNN) Deep Learning | - The proposed multimodal hybrid model showed improved performance with an accuracy of 95.66% |

| | | | | |
|--|---|--|---|---|
| <p>Classification of Gait Type Based on Deep Learning Using Various Sensors with Smart Insole [29]</p> | <ul style="list-style-type: none"> - Pressure Sensor Array - Acceleration Sensor Array - Gyro Sensor Array | <ul style="list-style-type: none"> - Walking - Fast Walking - Running - Stair Climbing - Stair Descending - Hill Climbing - Hill Descending | <p>- DCNN</p> <p>Deep Learning</p> | <p>- High classification rate of more than 90%</p> |
| <p>Deep Neural Network-Based Gait Classification Using Wearable Inertial Sensor Data [30]</p> | <ul style="list-style-type: none"> - 3-axis accelerometer - 3-axis gyroscope | <ul style="list-style-type: none"> - Athlete - Normal Foot - Deformed Foot | <p>- Convolutional Neural Network (CNN)</p> <p>Deep Learning</p> | <p>- Using the same model validation and evaluation method, up to 98.19% accuracy was achieved from the convolutional neural network-based classifier</p> |

Based on Table 2-3 above, for previous studies related with gait pattern using machine learning, the average accuracy was 82.5%. In other hand, for previous studies related with gait pattern using deep learning, the average accuracy was 94%. There is one specific study conducted by [31] to help with recovery planning using modern machine learning and deep learning techniques to give patients a safe gait evaluation covering all common gait-related parameters founds that bidirectional long short-term memory (Bi-LSTM), a deep learning classifier obtained an average of 90.54%, 90.41%, and 90.38% for precision, recall, and F1-score, respectively. On the other hand, 86.99%, 86.62%, and 86.67%, respectively, for SVM, a machine learning classifier. To conclude, based on the findings, Deep Learning is the best method to conduct gait pattern analysis for maximum accuracy. Deep learning have different types of algorithms such as Convolutional Neural Network (CNN) and Recurrent Neural Network (RNN) that are suitable with different types of data.

2.6.1 Convolutional Neural Network (CNN)

A type of feedforward mechanism neural network called a Convolutional Neural Network (CNN) can extract characteristics from input that has convolution structures. In contrast to the old feature extraction technique like Scale Invariant Feature Transform (SIFT), CNN eliminates the need for characteristics extraction manually [32]. CNNs are an effective kind of neural network that are frequently employed in tasks involving recognizing images. They are composed of one or more fully connected layers that employ the features extracted from the input image to produce predictions, after which a sequence of convolutional and pooling layers collect pertinent features from the image. CNN needs to first be trained on a sizable dataset of labelled images that contain the objects of interest in order to be used for image classification. Through replication and optimization, CNN

gains the ability to correlate the extracted features with the appropriate labels during training. Once trained, CNN may be used to predict new, unknown images by running the picture through the network and choosing the description with the greatest probability of accuracy [33]. Figure 2-5 shows the visualization of CNN layers that allow CNN to work.

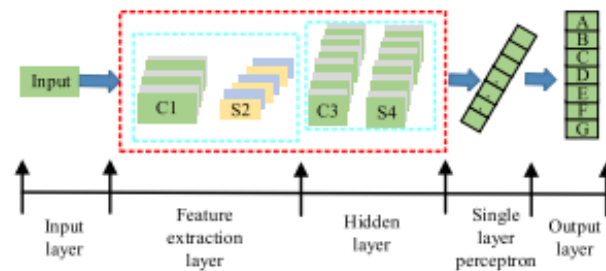


Figure 2-5 CNN layer

Three layers make up a convolutional neural network in general: the input layer, the hidden layer, and the output layer. The unprocessed initial picture is the input layer, the feature classification result is the output layer, and the hidden layer is a neural network layer with an intricate multi-layer nonlinear structure that consists of a convolution layer and a sub-sampling layer. Features in hidden layers are extracted and classified by convolutional neural networks. As a result, optimizing the single-layer perceptron and convolutional layer can enhance the precision of feature extraction and maximize the categorization result [34].

2.6.2 Recurrent Neural Network (RNN)

Recurrent Neural Network (RNN) employs the recurrence relation and learns via backpropagation via time. Every aspect in the sequence data is dependent on time. Sequence data is produced by numerous real-time applications, such as picture captioning, speech synthesis, speech recognition, and music production. For managing these kinds of data, RNN was created. By determining the short- and long-term sequence relationships between various data points, it effectively manages the sequence data. The RNN uses this

information to forecast by extracting the hidden pattern from these connections. RNN has different types of structures depending on number of inputs and outputs generated and is shown in Figure 2-6.

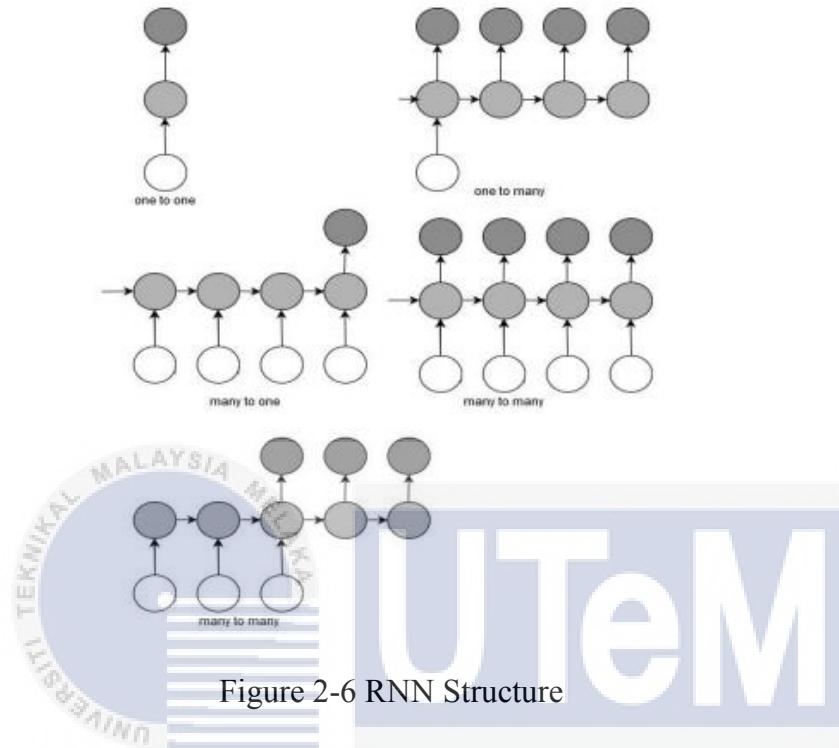


Figure 2-6 RNN Structure

RNN is interesting because it allows to work with lengthy vector patterns. The predictive accuracy of RNN can be enhanced by building the RNN's grid both horizontally and vertically. In figure 2-6, the RNN structure are divided into 4 categories which are one to one, one to many, many to one and many to many [35].

For motion prediction by using RNN, the way various body parts interact can make the traditional RNN structure inefficient for motion predictions [36]. This is where predictive accuracy of RNN can be enhanced by including components and coordinating functional units as an answer. The coordination unit examines how the various body parts interact, while the component unit studies the trajectory of a particular body part linked to a particular human stance. Figure 2-7 shows the base RNN structure that were used for motion prediction of a human.

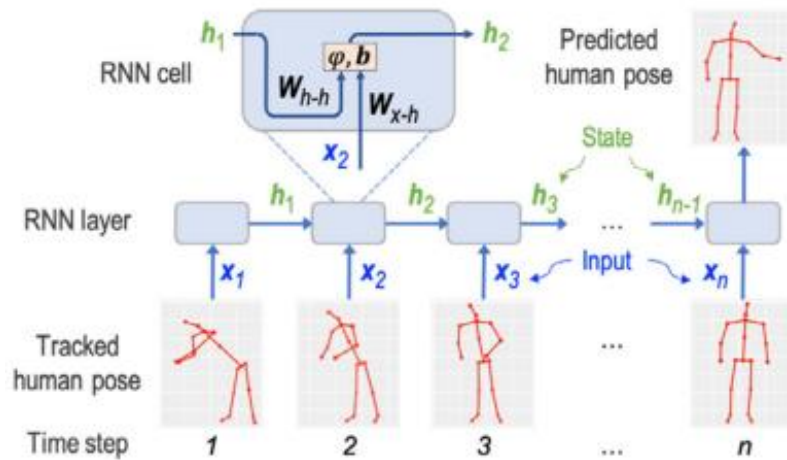


Figure 2-7 Motion prediction using RNN

For the enhanced RNN, every operational unit's network structure is derived from the standard RNN structure in figure 2-7. The difference is to depict a whole human body, a total of five separate parts (two arms, two legs, and one spine) and four coordination units (arm-arm, arm-spine, leg-leg, and leg-spine) were included. The Backpropagation algorithm trains the RNN structure with operational components collectively. Figure 2-8 shows the enhanced RNN structure that were derived from base RNN structure for motion prediction of a human.

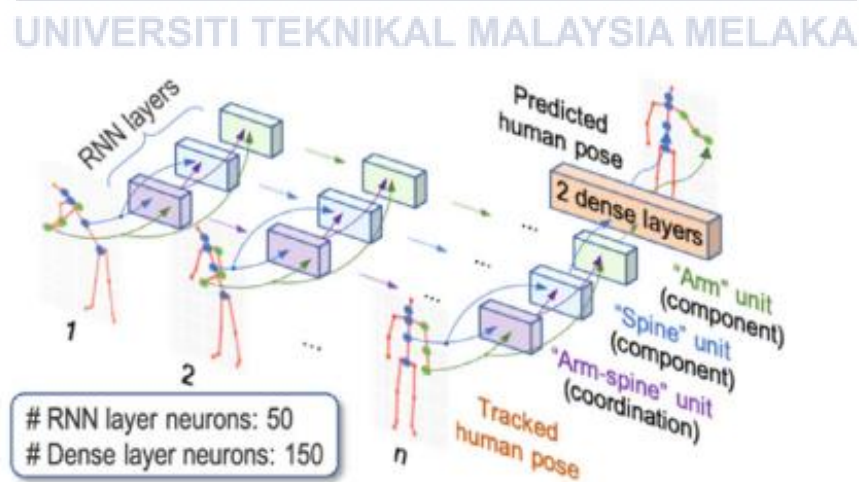


Figure 2-8 Enhanced RNN structure for motion prediction

Reducing prediction error, such an improved network structure makes it possible to forecast the human motion trajectory more accurately in the context of both its own history

and the interactions between the various body parts. Contrary to the RNN structure without operational components, there has been a roughly 40% decrease in the mean divergence between the predicted and actual locations of body joints [36].

2.7 Comparison Between Unimodal and Multimodal

In this study, multimodal data were used to classify gait and posture patterns. This decision were made based on past studies that have been conducted using unimodal and multimodal data. Table 2-4 shows the comparison between unimodal and multimodal data that supported the decision to choose multimodal data for this study.

Table 2-4 Comparison between unimodal and multimodal data

| Unimodal | Multimodal |
|--|--|
| <p>Have a number of flaws that lower the system's accuracy such as:</p> <ul style="list-style-type: none"> • noisy data • non-universality • intra-class variance • inter-class similarity. [37] | <p>Using the detection and processing of two or more physiological or behavioral features, have shown to considerably increase the success rate of identification and verification. [37]</p> |

To further strengthen the finding from Table 2-4, a study was conducted between unimodal and multimodal for biometric authentication. It is found that for multimodal authentication of fingerprint and face, the training accuracy is 99% while for unimodal authentication of fingerprint and face, the training accuracy would be 97% and 98% respectively [38].

CHAPTER 3

METHODOLOGY

3.1 Introduction

This chapter will discuss the thorough approach used to categorize the gait pattern into three classifications: walking straight, turning right, and walking left on a hallway. A means of determining the project's implementation from start to finish is research methodology. The project's implementation will also be covered in full in this chapter, along with an explanation of how each step is put together. The three stages of this project are data classification, data processing and data pre-processing. FYP1 will complete the data pre-processing and data processing, and FYP2 (final year project 2) will carry out the remaining one phase. Figure 3-1 shows the overview flowchart of the methodology that has been and will be conducted in FYP 1 and FYP 2.

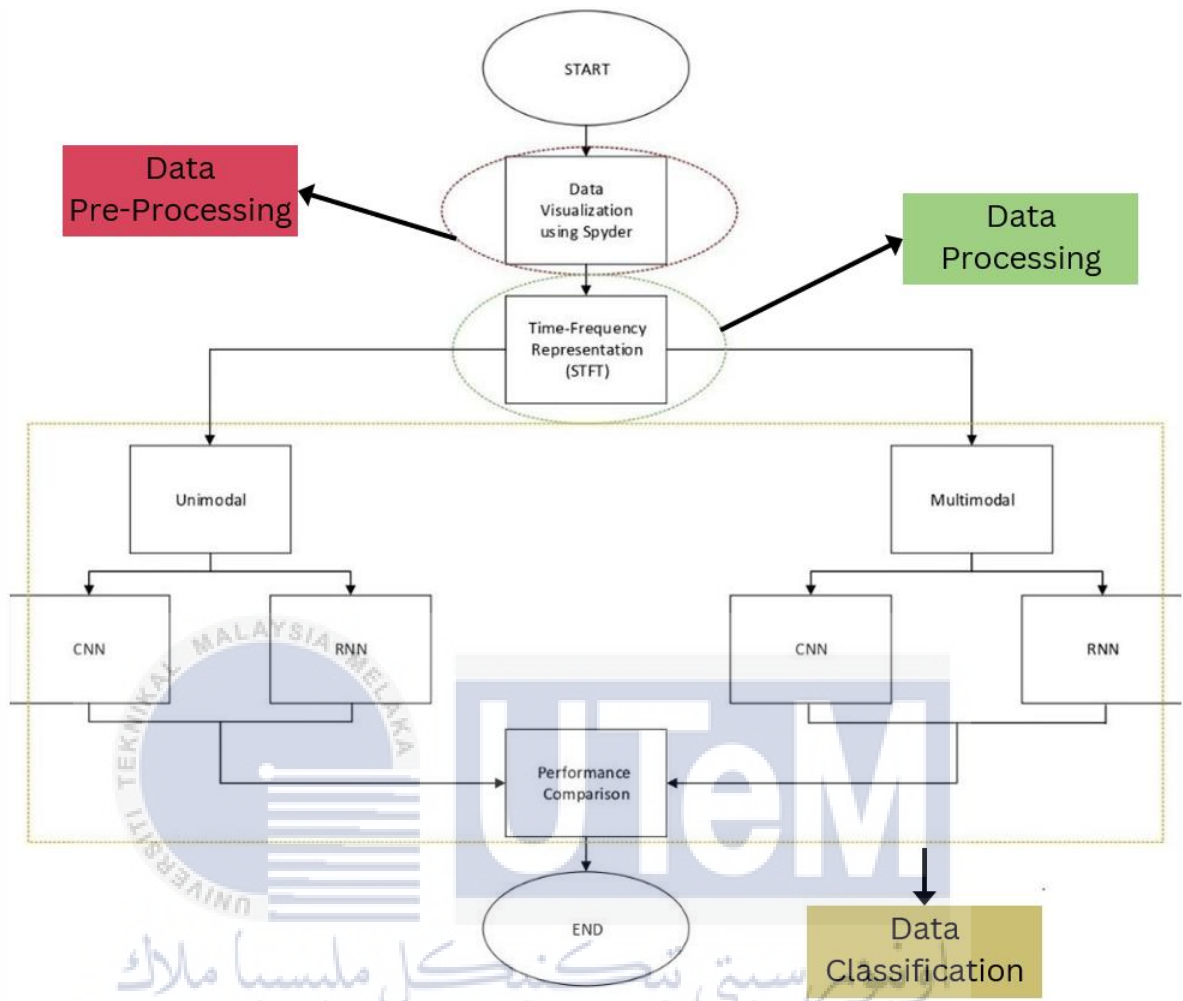


Figure 3-1 Overview of methodology

3.2 Dataset Description

The dataset that were used in this study were collected based on different walking situations. The datasets were contributed by Manuel Palermo to Physionet. For this study, the situations are walking straight, turning left and turning right on a corridor. The data were collected from 14 healthy participants which are comprised of 10 men and 4 women which weight are in 69.7 ± 11.4 kg range, height in 172 ± 10.2 cm range and age in 25.4 ± 2.31 years-old range. The participants were chosen based on some specific criteria such as they exhibit normal mobility and have no previous record of anomalies in their clinical condition, current state of complete control over posture, current height in centimeters from 150 to 190, are at least 18 years old and given permission in writing to take part in the study.

3.3 Data Collection Scenarios

The steps involved in the experimental protocol were as follows: first, the anthropometric measurements of the participants were taken and entered into the MVN Analyse in order to adapt the software's biomechanical model (MVN BIOMECH) to their physiognomy; second, the MVN BIOMECH was calibrated according to the manufacturer's instructions, guaranteeing the accuracy of the calibration for every subject. Another IMU was mounted on a stick during the calibration processes, and it was relocated to the upper camera to ensure consistent orientation throughout the trials when the calibration was complete.

The following types of data were gathered: i) kinematic data, which included the orientation, velocity, and acceleration of segments; the angle of joints; and the free acceleration, magnetic field, and orientation of sensors. These were obtained with the

MVN software at 60 Hz; and ii) 30 frames per second (fps) depth pictures taken by the walker's embedded cameras. A hardware trigger was used to synchronize the time of all the data. Figure 3-2 shows how the data collection scenarios was set up for a participant.



Figure 3-2 Gait and posture data collection setup for participants

UNIVERSITI TEKNIKAL MALAYSIA MELAKA

3.4 Ethics and Safety of Data Collection Scenarios

The Helsinki Declaration and the Oviedo Convention were followed in the data collecting process, which was carried out in accordance with the Ethics Committee in Life and Health Sciences' (CEICVS 063/2021) ethical guidelines. By protecting the rights of the participants, private personal information was maintained and is not included in this dataset.

It was advised that participants wear athletic shoes and long pants to avoid unnecessary injuries while doing the data collection scenarios as it involves walking through different situations along the corridor. The full body inertial motion tracking system MTw Awinda was used to monitor each participants' gait and posture data. Seventeen IMUs were strapped onto each participants' head, shoulders, chest, arms, forearms, wrist, waist, thighs, shanks and feet. To determine the orientation of the camera with respect to the MVN world axis, an extra IMU was mounted to the upper camera of the walker. This was done to give clean data relating to the camera without revealing the position of the sensors. The researchers placed the sensors in accordance with the manufacturer's instructions, reducing the possibility of errors resulting from incorrect sensor placement.

3.5 Data Pre-processing

Timestamp files that were captured during acquisition with the walker's embedded software are used to synchronize temporally data from the inertial motion tracking and the depth images. Each modality's matching temporal indexes were stored in a ".csv" file, which retains all of the raw samples acquired and makes data selection simple when needed.

All of the data from the open-source database were downloaded. In order to further understand and visualize the posture and gait data, Python Spyder were used. The coding for visualizing the data were given in the database. Figure 3-3 shows the overview flowchart of the coding to visualize the gait and posture of each participant walking.

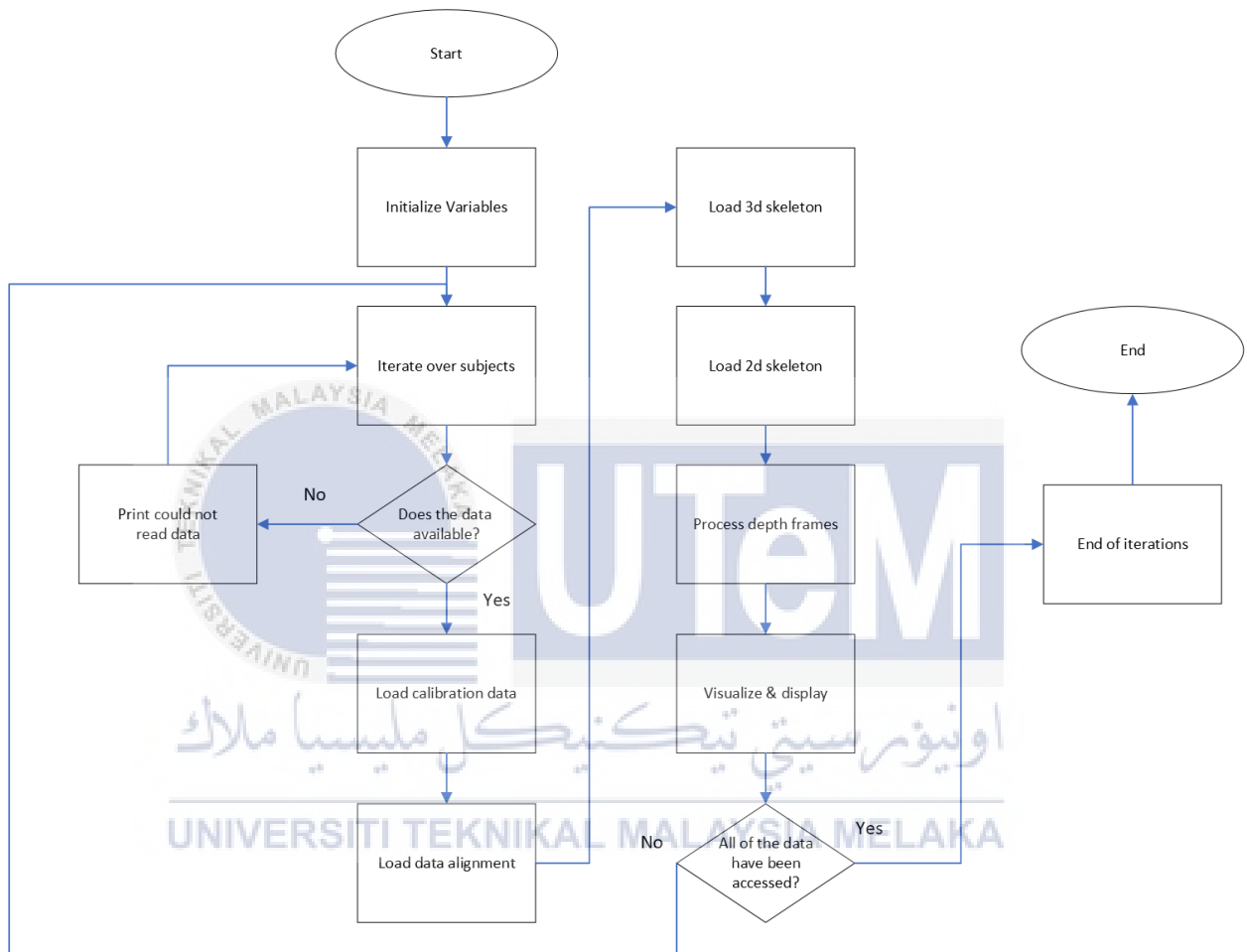


Figure 3-3 Overview flowchart of data-preprocessing coding

The coding starts with initializing all the variables. All the library that is required and compulsory for the code to run is imported here. The examples of the library that are required for this code to run are NumPy, Pandas and OpenCV (cv2). NumPy is a Python language library that supported complex matrix structures and provide mathematical algorithms to manipulate mathematical components. Next, Pandas is an information processing and management tool. It offers efficient formats for managing organized

information while OpenCV is a library that helps with artificial recognition. Processing images and videos are one of its common uses.

Next, the coding moves to the iterate over subjects' part. This study involves 14 participants that walking straight, turning right and left along a corridor. All the data files are named with the participant number and walking condition identification. So, to ensure that the files will be go through one by one, these lines of coding are important so each participant with each walking condition files can be visualized and not one of it will be missed.

After that, the coding will move to a decision-making process which includes checking the data availability. If the data for a certain participant with a certain walking could not be viewed due to error of the data or corrupted files, the coding will print "Could not read data from: participant00 | straight". It contains the exact information of which participant and the conditions of walking file that could not be processed. Once the message is generated, it will move back to the iterate over subjects' process which means it will process the next participant or walking condition file. If the data for the participant and walking condition can be accessed, it will move to the next part which is the load calibration data.

In load calibration data process, it reads the calibration information of the extrinsic and intrinsic for each participant with walking conditions files. In extrinsic information, it reveals the positional link between various cameras while for the intrinsic information, camera's unique properties such as the lens' focal length and primary spot are revealed. The imported calibration data is subsequently used in later code segments for additional analysis.

Moving on, load 3d skeleton process helps to obtain data regarding each participants' joint movements in three dimensions such as the shoulders and knees movements. This is where the Pandas library helps to read the complex dataset and process it. This part of coding helps to know the dynamics of the participants' body movement in 3 dimensions over time. The information is arranged and ready for additional examination or be displayed. For the 2d skeleton process, it works the same way as the 3d skeleton process works but the difference is only the 2d skeleton data are in x and y axis whereas the 3d skeleton data are in x, y and z axis.

Furthermore, the code proceeds to process depth frames data. The depth frames data were load and this is where the OpenCV library comes in handy. OpenCV read depth images that were taken by cameras at certain frames and the images were then processed. This process is also processed and transformed to a floating-point format so that depth information may be handled more precisely. After that, the depth frames are ready for visualization in the program's main loop.

Moreover, visualizing and displaying data involved improving and displaying the analyzed data in a visual format. To improve the exposure of the visualization, the brightness of the frames was changed, and the visualization are separated in two different windows which shows the posture frames and the gait frames. This graphic depiction helps to understand the participants' motions during the examined frames. Once all files of each participant with different walking conditions have gone through, the iterations will stop, and the process will end. If not, the code will bring back to iterate the next participant with different walking conditions file until all the files have been accessed.

3.6 Data Processing

TFD characteristics have been selected for signal processing in this project. This is due to the domain's ability to get beyond limitations in the frequency and time domains. Next, in order to extract the crucial information from the physiological signals, TFD requires modifying the time and frequency resolution.

Data for gait and posture aligned with time were chosen as Time Frequency Representation (TFR) requires time aligned data. The Time-Frequency Representation (TFR) will be obtained using Short Time Frequency Transformation (STFT) method using Python Spyder software coding in Python. After setting the overlap between adjacent segments to 50%, the TFR is produced. The overlap was set at 50% because it makes it easier to see how easily the components are changing from moment to the next. Table 3.1 shows the gait and posture data for participant 1 when turning right that are aligned with time.

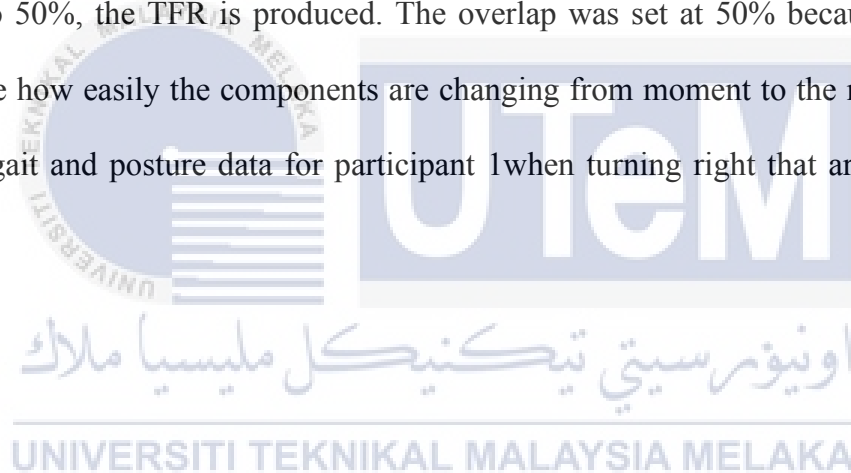


Table 3-1 Gait and posture depth data for participant 1 aligned with time

| Time(s) | Posture Data(mm) | Gait Data(mm) |
|----------------|-------------------------|----------------------|
| 0 | 14 | 14 |
| 1 | 15 | 15 |
| 2 | 17 | 16 |
| 3 | 18 | 17 |
| 4 | 19 | 18 |
| 5 | 20 | 19 |
| 6 | 21 | 20 |
| 7 | 22 | 21 |
| 8 | 23 | 22 |
| 9 | 24 | 23 |
| 10 | 25 | 24 |
| 11 | 26 | 25 |
| 12 | 27 | 27 |
| 13 | 28 | 27 |
| 14 | 29 | 28 |
| 15 | 30 | 30 |
| 16 | 31 | 30 |
| 17 | 32 | 32 |
| 18 | 33 | 33 |
| ... | ... | ... |
| ... | ... | ... |
| 508 | 523 | 523 |
| 509 | 524 | 524 |
| 510 | 525 | 525 |

It can be seen that in Table 3-1, the gait and posture data for participant 1 starts with 0 seconds and ends at 510 seconds. It shows that participant 1 takes about 510 seconds to finish walking turning right on a corridor. Other participants exhibit roughly about the same time to finish the walking on the same condition. These files were used to generate TFR using the STFT method.

For generating the TFR, Spyder software were once again used, and the coding is also in Python language. The STFT method were included in the coding as well as the visualization of the TFR. Figure 3-4 shows the overview flowchart of the coding to generate Time Frequency Representation (TFR) using Short Time Fourier Transformation (STFT) method.

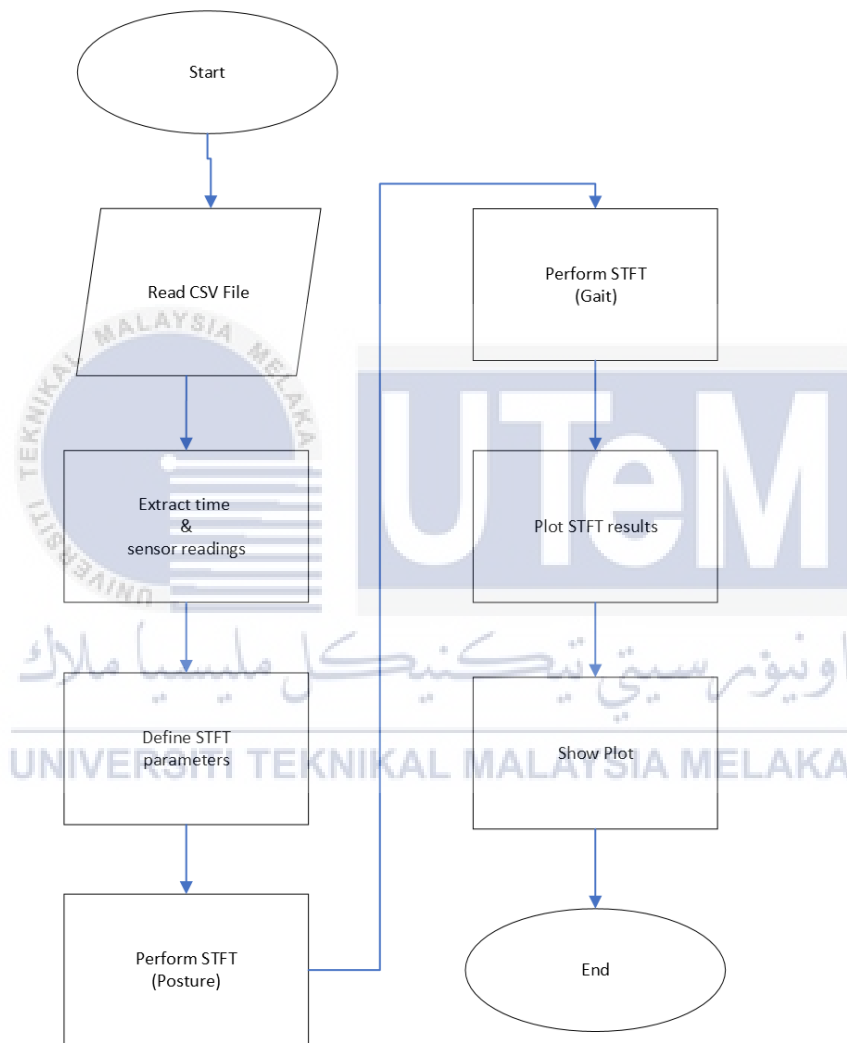


Figure 3-4 Overview flowchart of data processing coding

Based on the flowchart in Figure 3-4, the coding starts with extracting the data that contains time, posture data and gait data as shown in Table 3-1. The time, posture and gait data are held into an array by NumPy library that have been imported. The data is then separated to 3 columns in the array with time data in array 1, posture data in array 2 and

gait data in array 3. These separated arrays store the corresponding temporal and sensor reading data during the moment. The exact information elements needed for further data processing and analysis which in this case, are for Short Time Fourier Transform (STFT).

Moving on, the code proceeds to define the STFT parameters. It analyses the data frequency shifts over brief short periods of time. The variables used in this code are “overlap = 32” and “window size = 64”. The choice between frequency and time resolution is influenced by the “window size”, which establishes the number of samples considered in every evaluation window. As for the overlap parameter, it affects the amount of overlap between time sections by defining the total amount shared between successive windows.

Next, the code generates the TFR of STFT for posture and gait signals by using the SciPy library that have been imported in the earlier part of the code. The SciPy library helps to capture the frequency information of the signals during brief overlapping time frames. The previously set factors like “window size” and “overlap” help to customize the analysis to the specifics of the sensor information.

Furthermore, for plot STFT results this procedure comprises of visualizing the posture and gait sensor readings from the outcome of STFT procedure earlier. The code generates two subplots each showing a TFR diagram for posture and gait pattern respectively which contains the shifts of frequency over time. The plots help the examination of the dynamic properties of the posture and gait pattern by providing a thorough visual depiction of the time changes in the frequency domain. It also includes axis labels, titles and color bars.

3.7 Data Classification

For data classification, two deep learning algorithms which are Convolutional Neural Network (CNN) and Recurrent Neural Network (RNN) were used in order to get the accuracy percentage for the classification of gait and posture pattern. STFT diagrams that were obtained from data processing method earlier were used for this part. For multimodal data, both gait and posture STFT diagram were fed to the selected deep learning algorithms while for unimodal data, only gait STFT diagram were used. In order to prevent inadequate quantity of training data or an unequal distribution of classes within the datasets, an approach called “data augmentation” were used to address the issue [39]. For this research, the STFT diagrams were rotated to 0° , 90° , 180° and 270° for the data augmentation approach [40]. Furthermore, to avoid dataset overfitting issue, early stopping approach have been used in this research [41]. Matlab were used for this data classification method as it helps to build the structure of the deep learning algorithms and produce the accuracy percentage.

Unimodal and multimodal datasets for CNN and RNN algorithm requires different coding, but all of the coding stands with the same foundation. Figure 3-5 shows the overview of the coding of both unimodal and multimodal datasets for CNN and RNN algorithm.

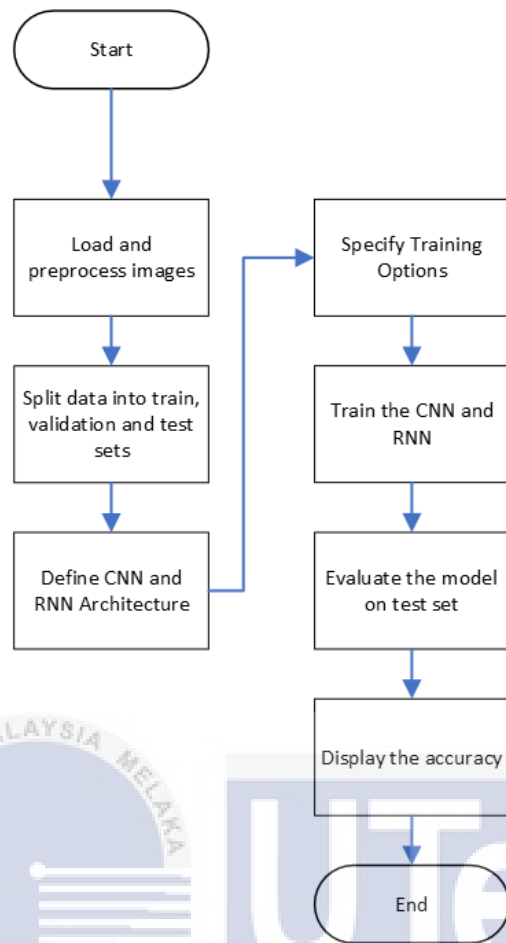


Figure 3-5 Overview flowchart of data classification coding

The STFT diagrams that contained the gait and posture data were organized in folder according to its classification, turning left, turning right and walking straight for both multimodal and unimodal data. So, based on the flowchart in figure 3-5, the coding starts with load and preprocess images. This part requires naming the classes, initializing empty arrays for each class, defining the path to the primary dataset folder holding subdirectories for each class, setting the target image size and creating a random seed for reproducibility.

Next, in splitting data into training, validation and test sets, the datasets for CNN were divided in percentage for training, validation and tests. The exact percentage for the division is 80% for training, 10% for validation and 10% for tests. Which means for multimodal and unimodal datasets, from a total of 168 pictures, 134 pictures were used for

training, 17 for validation and 17 for testing. For RNN, the datasets were divided into 80% for training and 20% for validation.

Moving on to define algorithm architecture, for CNN, a 3x3 convolutional layer with 8 filters and the same padding to maintain the three dimensions comes after the image input layer. The feature maps are then down sampled using max-pooling layers with 2x2 windows and a stride of 2. This procedure is performed using a different 16-filter convolutional layer. The network is trained with a specific learning rate and number of epochs using the Adam optimizer. The precision of the network's output is assessed using a different test set. While for RNN, A sequence input layer, a flatten layer (to guarantee that the input size is compressed), an LSTM layer to analyze sequential information, a fully connected layer, a SoftMax layer, and a classification layer make up the RNN architecture. The time-dependent relationships between successive inputs are captured by the LSTM layer.

For the specify training options, parameters like learning rate, epochs, batch size and validation data were set in this part. The parameters were fine tuned in order to gain the highest accuracy possible for every situation. Together, these choices shape the neural network's training process and its ability to identify patterns in the data.

Furthermore, in the training the algorithm part, for CNN, training data (X_{train}) and matching labels (Y_{train}) are sent into the CNN to train it. In order to minimize the gap between its predictions and the actual labels, the network modifies its internal parameters such as weights and biases during training. This iterative process known as optimization takes place over a number of epochs, or one run of the complete training dataset. The designated training settings, which include selecting the optimizer, learning rate, and mini-batch size, direct the training process which were set in the step before. The network gradually becomes better at identifying patterns in the input data as training goes

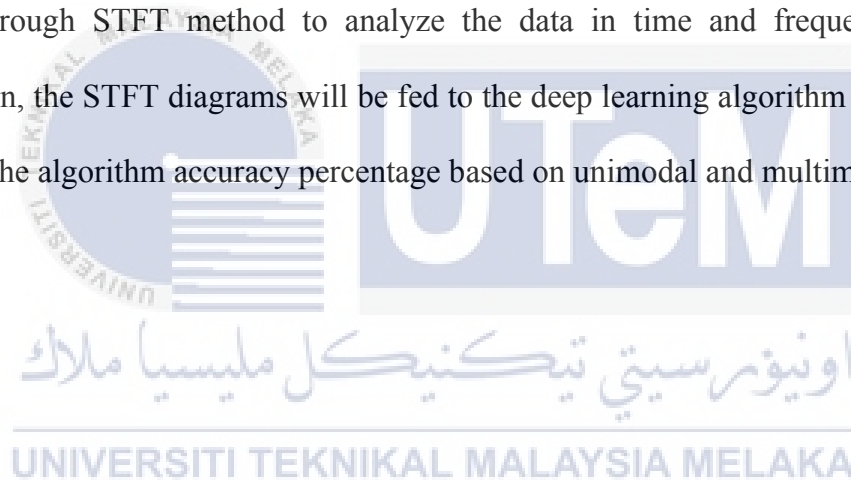
on, which eventually results in a model that can correctly categorize unseen images. While the difference in RNN algorithm is the RNN algorithm prepares the sequences, splits the data into training and validation sets, then trains the model with predefined training choices. It assesses the model's effectiveness using an independent validation dataset.

On the evaluate the model on test set, The model is trained on the training dataset, and after that, its performance is assessed on the test set, which is a different set of data that the model did not encounter during training. The purpose of this evaluation is to determine how effectively the trained model applies to fresh, untested data. Images (X_{test}) and the true labels (Y_{test}) that go with them make up the test set. The test images are predicted using the trained model, and the accuracy of the model is assessed by comparing the predictions with the true labels.

Lastly, on the display the accuracy part, by dividing the total number of test photos by the number of accurate predictions, the code determines accuracy. This ratio, which is given as a percentage, shows how well the model classified the test images. By demonstrating accuracy, one can gain important understanding of the model's performance, as well as how effectively it generalizes to new, untested data and whether it is suitable for real-world applications.

3.8 Summary

The deep learning classifier that were chosen, RNN and CNN were chosen for their suitability to work with this study's data which are images. The database utilized for this project came from Physionet. which Manuel Palermo, the creator, contributed. Three essential steps referred to as data pre-processing, data processing and data classification are required for any physiological information. For this study, the data pre-processing were done to visualize the gait and posture pattern of each participant in 3d to help understand of how every participant walks during different walking situations. For data processing, TFR diagram of gait and posture data for each participant will be generated using Spyder software through STFT method to analyze the data in time and frequency. For data classification, the STFT diagrams will be fed to the deep learning algorithm in order to test and obtain the algorithm accuracy percentage based on unimodal and multimodal data.



CHAPTER 4

RESULTS AND DISCUSSION

4.1 Introduction

This chapter, which is organized into three sections, offers the findings and discussions from the techniques described in the preceding chapter. The data can be visualized and further analyzed during the pre-processing step to comprehend the participant's posture and steps while walking in various situations. In the data processing stage, the time frequency representation will be obtained through the application of the STFT method. The final step will compare the two deep learning models which are CNN and RNN in order to recognize the posture and gait patterns of walking ahead, turning right, and left along a corridor.

4.2 Data Pre-Processing

Figure 4-1 and 4-2 are the representation of the visualized posture and gait pattern that were generated from the coding in methodology. Each participant's gait and posture pattern data in .csv file are used through Spyder software. The gait and posture pattern are further understood and gait pattern (walking straight, turning right and left on a corridor) can be distinguished by watching the visualized data.

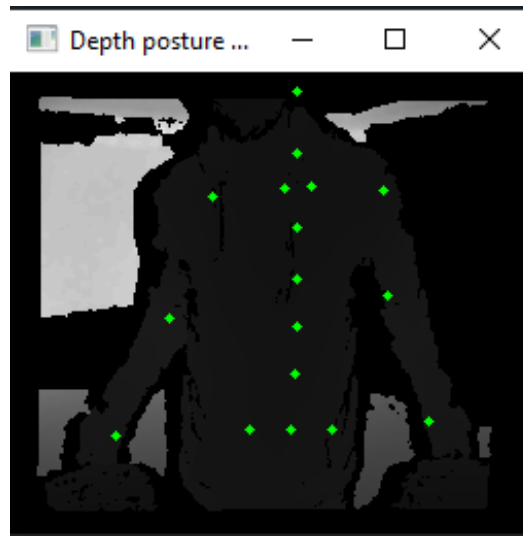


Figure 4-1 Participants' posture data visualization while walking

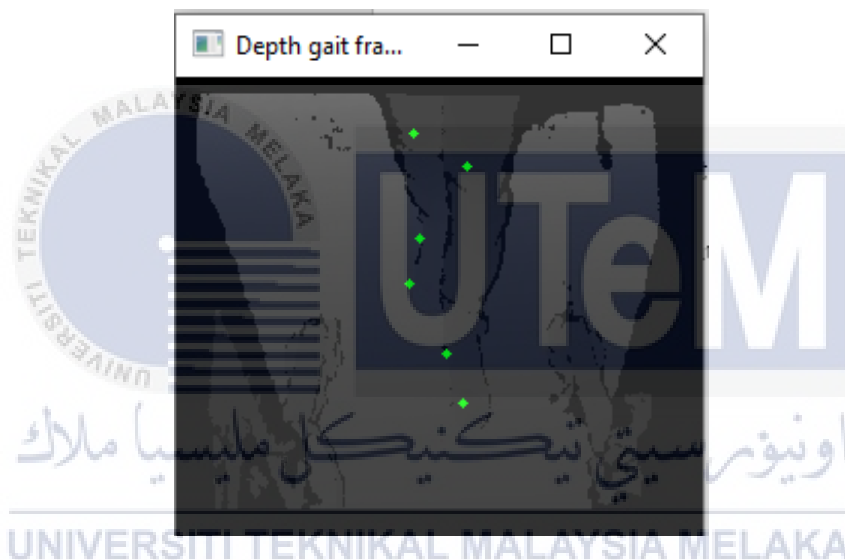


Figure 4-2 Participants' gait data visualization while walking

Each of the participants' gait and posture visualization of gait and posture while walking through different conditions (walking straight, turning right and left) were recorded and analyzed. It does help with understanding the gait pattern and processing the data in the next part which is data processing.

4.3 Data Processing

In data processing, a feature extraction will be extracted from the data. In this project, the important part is the TFR diagram through STFT method. Figure 4-3, Figure 4-4 and Figure 4-5 below shows the STFT diagram for participant 1 turning left, turning right and walking straight. These TFR diagrams will act as the dataset and all of participants TFR will be fed into the deep learning classifier. Other examples of STFT diagram for other selected participants will be shown in Appendix A.

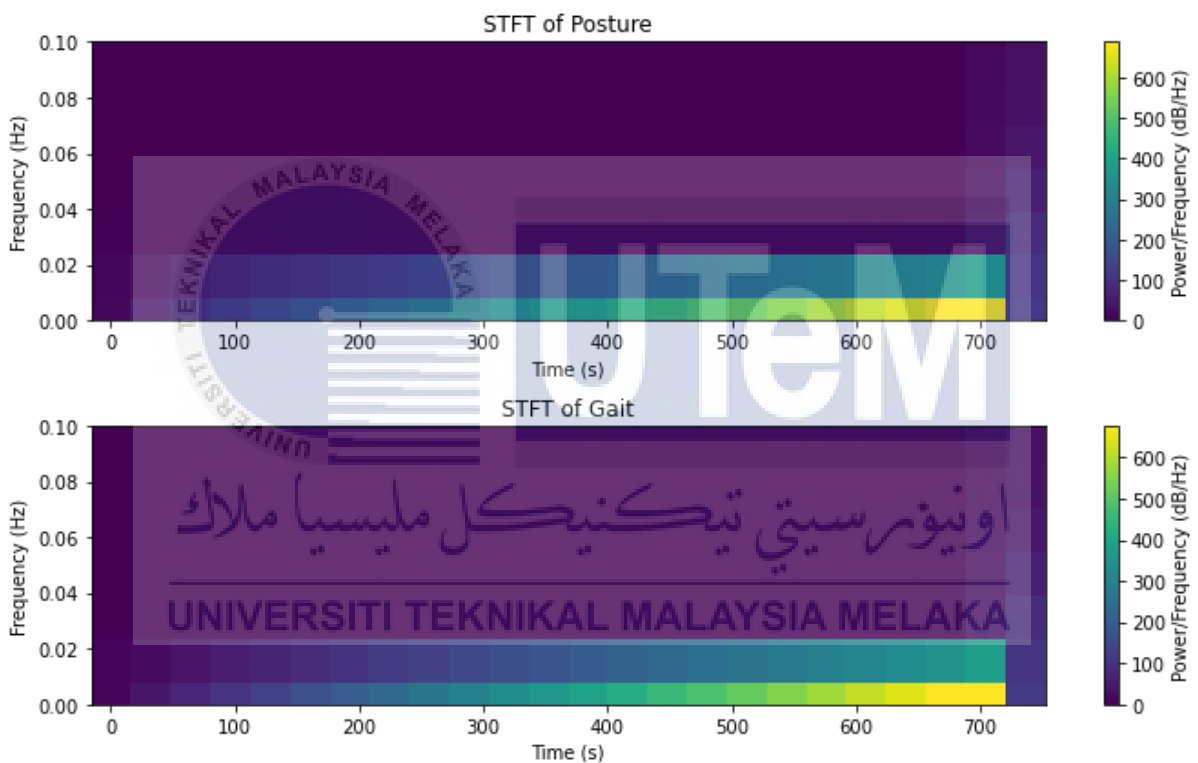


Figure 4-3 TFR diagram for participant 1 turning left

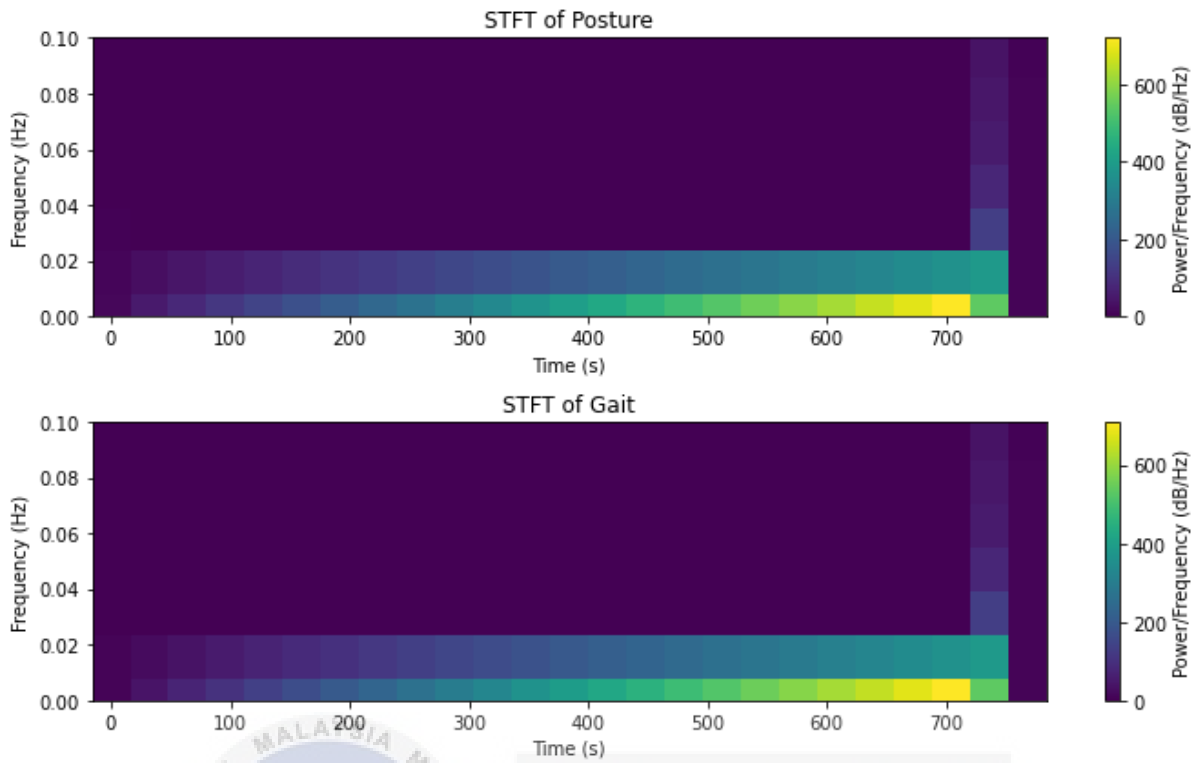


Figure 4-4 TFR diagram of participant 1 turning right

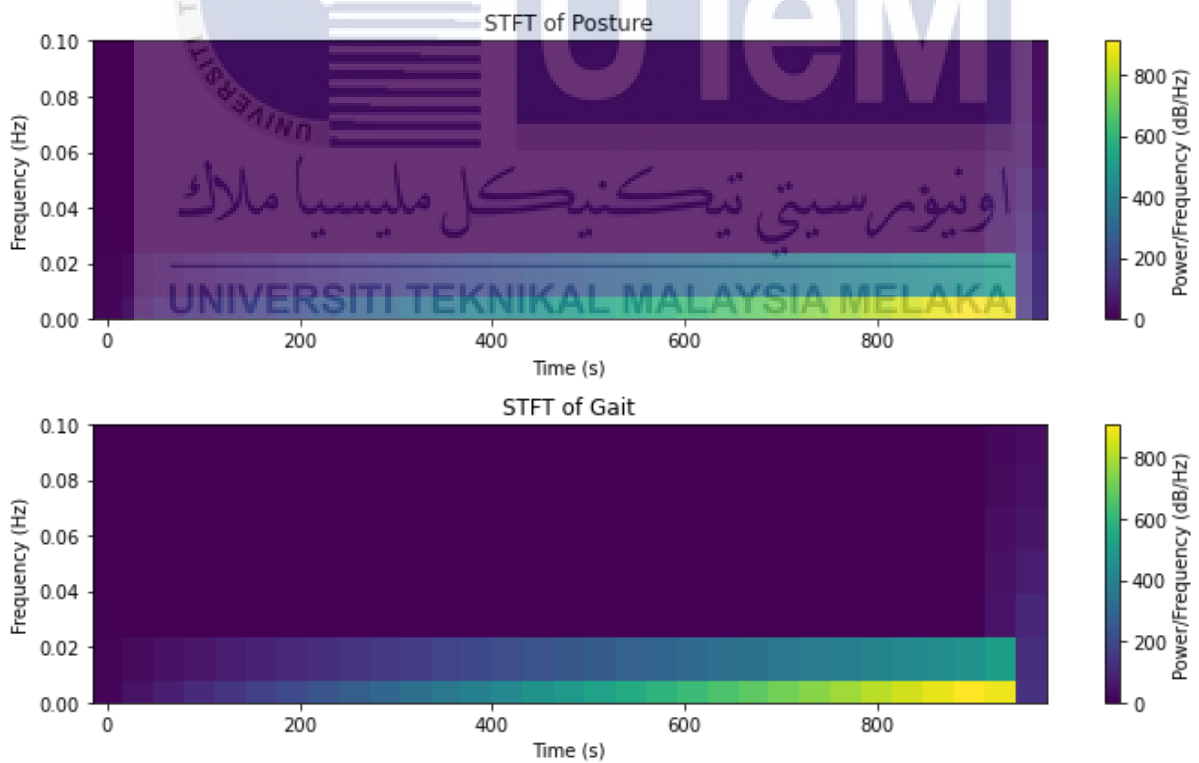


Figure 4-5 TFR diagram of participant 1 walking straight

The y-axis of the STFT diagram are represented by the frequency of the signal and on the x-axis, it is represented by the time of how long the participant finished walking. The signal's level of energy at a specific frequency and time is represented by the color intensity. The highest amplitude are represented by the yellow color while the lowest amplitude is represented by the purple color.

From the STFT diagrams above, the amplitude gets higher over time because of the increased movement of participant walking over time. Figure 4-3 shows the TFR diagram of participant 1 walking turning left on a corridor. It can be seen that the obvious changes are located at the end of the diagram. During frequency around 0.02 Hz and time around 700 seconds, power/frequency color waves that occurred there are around 400-600 dB/Hz and right after that the power/frequency color drops around 100 dB/Hz.

For Figure 4-4, it shows the TFR diagram of participant 1 walking turning right on a corridor. This diagram also exhibits obvious color changes at the end of the diagram. Different from participant walking turning left explained before, for Figure 4-4 during frequency around 0.02 Hz and time around 750 seconds, the power/frequency color waves that occurred there are around 300-500 dB/Hz only compared to 400-600 dB/Hz in Figure 4-3 when participant turning right. Right after that, the power/frequency color drops to 0 dB/Hz.

Lastly, for Figure 4-5, it shows the TFR diagram of participant 1 walking straight and like 2 of the situations of walking before, the obvious color changes occurred at the end of the graph as well. During frequency around 0.02 Hz and time around 900 seconds, the power/frequency color waves that occurred there are around 650-850 dB/Hz.

To conclude, walking straight exhibit the highest power/frequency color waves compared to turning right and left along a corridor. This some condition might happen based on a few reasons. One of it is it might be because of efficiency in energy use while

walking straight. Unlike turning left or right, walking straight uses fewer motions of the body and feet and less muscles stimulation are needed. This might result in increased effectiveness of producing low frequency vibrations that helps to increase the power/frequency value. These low frequency waves could be the result of walking-related foot impact with the floor or vibrations around the body while walking.

4.4 Data Classification

In data classification, CNN and RNN deep learning algorithms were used. Figure 4-6, Figure 4-7, Figure 4-8, Figure 4-9 shows the result for this data classification.

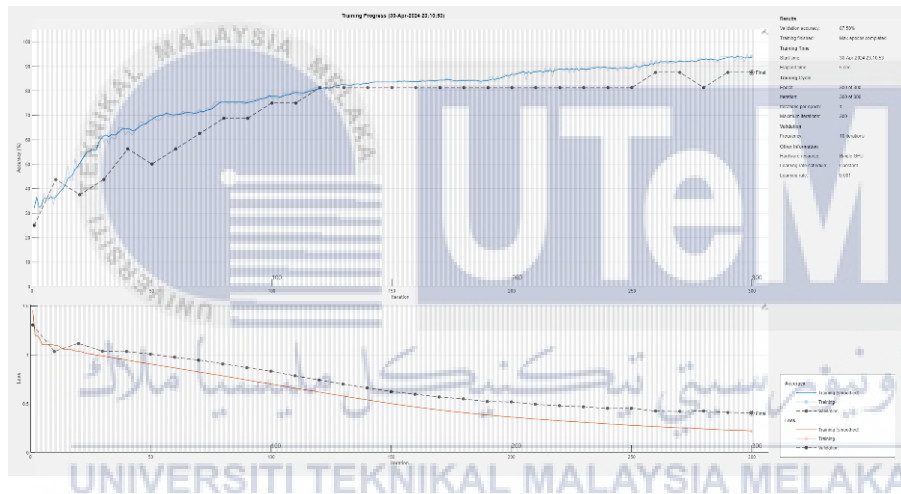


Figure 4-6 CNN Multimodal Classification Accuracy Percentage

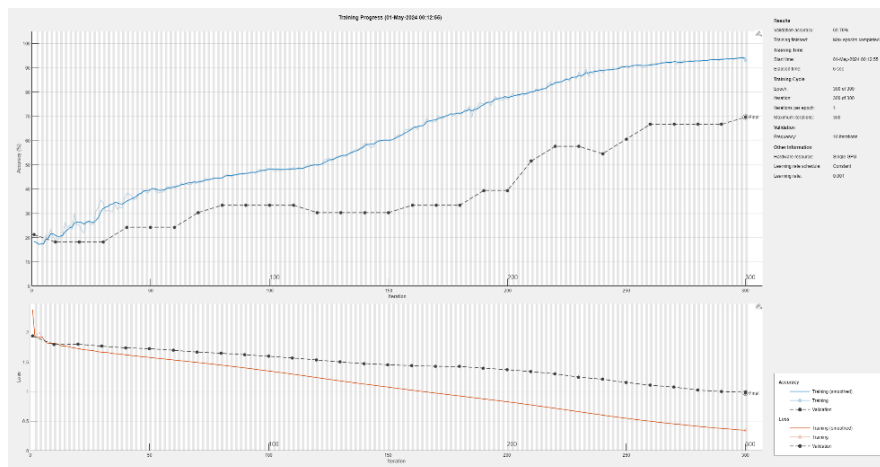


Figure 4-7 RNN Multimodal Classification Accuracy Percentage

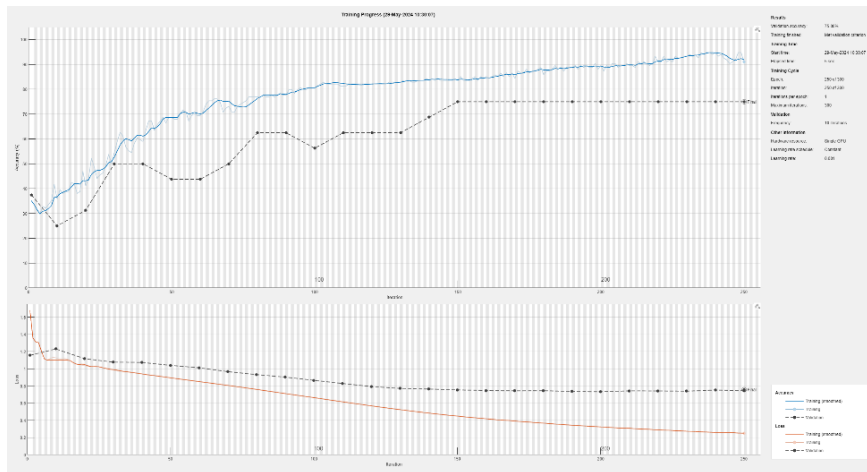


Figure 4-8 CNN Unimodal Classification Accuracy Percentage

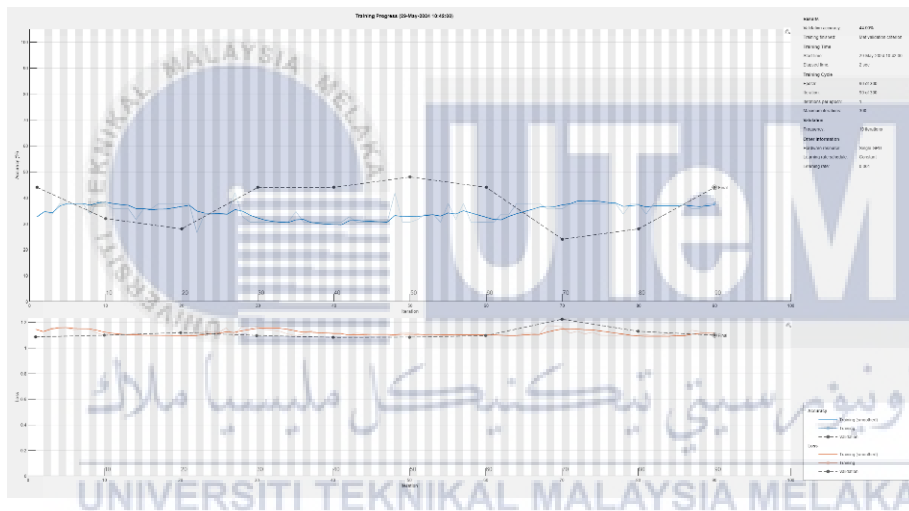


Figure 4-9 RNN Unimodal Classification Accuracy Percentage

For Figure 4-6, for CNN with multimodal data, as the training time comes to a finish, the training accuracy steadily rises and settles at about 80%. Validation accuracy improves but varies before levelling off at about 87.50%. A steady drop can be seen in the training loss and act as an indication that the model is learning well. The validation loss exhibits small swings but also reduces, indicating that the model's performance on the validation set may vary. After more than 250 cycles of training and validation, the model's ultimate validation accuracy was 87.50%. The set cycles was actually 300 cycles but

because of the early stopping method that has been implemented, the cycle stops at 250 cycles only as the model does not show any improvement anymore. Excellent accuracy is indicated by both training and validation metrics, and the model converges well within the allocated iterations.

For Figure 4-7, as for RNN with multimodal data, as the training time comes to a finish, the training accuracy increases steadily and settles at 50%. Validation accuracy first rises but then varies greatly before stabilizing at roughly 69.70%. A steady drop in training loss shows that the model is adapting and getting better. Validation loss initially declines but varies, suggesting that the model's performance varies on the validation set. The system uses full 300 cycles which means the system shows improvement until the end of the cycle.

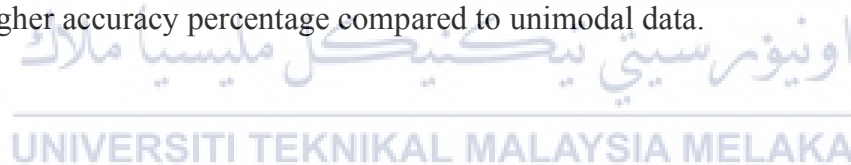
For Figure 4-8, as for CNN with unimodal data, training accuracy increases gradually with some swings before stabilizing at 85%. A stronger increasing trend is shown by the smoothed training accuracy line (blue), which indicates steady learning. Although it fluctuates at first, especially in the later stages of the iterations, the validation accuracy improves immediately. By the end of the training phase, it stabilizes at roughly 75%, demonstrating the model's capacity to generalize to fresh data. The system only uses 250 cycles out of 300 cycles as it stops improving around 250 cycles.

For Figure 4-9, as for RNN with unimodal data, the precision of training exhibits a tendency of fluctuation followed by a slow increase, indicating that the model is learning but rather unstable. The training loss shows some tiny variations but remains rather constant, suggesting that the model is learning over rounds but not improving much. The system only uses 90 cycles out of 300 cycles as it stops improving around 90 cycles only.

Table 4-1 Comparison between CNN and RNN also multimodal and unimodal data

| Description | Accuracy Percentage (%) |
|--------------------|--------------------------------|
| CNN (Multimodal) | 87.5 |
| CNN (Unimodal) | 75.0 |
| RNN (Multimodal) | 69.7 |
| RNN (Unimodal) | 44.0 |

In Table 4-1, comparison between CNN and RNN also multimodal and unimodal data were shown. CNN models exhibits a greater result in accuracy compared to the RNN models. CNN with multimodal and unimodal data produces accuracy of 87.5% and 75% respectively while RNN with multimodal and unimodal data produces accuracy of 69.7% and 44%. From this research, it is known that CNN are the better algorithm to conduct gait and posture pattern classification compared to RNN algorithm and multimodal data produces higher accuracy percentage compared to unimodal data.



CHAPTER 5

CONCLUSION AND RECOMMENDATIONS

5.1 Conclusion

In the proposed work, the representation of camera and accelerometer data is represented in Time Frequency Representation images by using the STFT method. Deep learning and multimodal data are used to classify the images according to various walking situations, and it is investigated whether this approach is more effective for classifying posture and gait patterns than traditional features. Using Spyder software, data from fourteen people were split to obtain the Time Frequency Representation for three different walking scenarios: straight ahead, turning left, and right on a hallway. Based on result of TFR diagram using STFT method for participant 1, when participant 1 walking straight exhibits the highest power/frequency reading compared to reading when participant 1 turning right or left in a corridor. This is because walking straight uses less energy and requires less muscle activation that allows effectiveness in producing low frequency vibrations that leads to higher power/frequency reading. For the accuracy of the algorithm which are CNN and RNN work based on multimodal data, CNN with multimodal data produces the highest accuracy percentage which are 87.5%, followed by CNN with unimodal data that produces accuracy of 75%. Both RNN with multimodal and unimodal data produces accuracy percentage that are lower which are 69.5% and 44% respectively.

5.2 Future Works

For future research, adjustments other than early stopping and data augmentation which have been done in this research can be made. There are other adjustments that can be made which are dropout regularization and learning rate adjustments. These adjustments can be investigated in the near future to ensure that the accuracy percentage can be pushed higher and nearer to 100%.



REFERENCES

- [1] W. Zeng *et al.*, ‘Classification of asymptomatic and osteoarthritic knee gait patterns using gait analysis via deterministic learning’, *Artif Intell Rev*, vol. 52, no. 1, pp. 449–467, Jun. 2019, doi: 10.1007/s10462-018-9645-z.
- [2] B. Guelta, R. Tlemsani, S. Chouraqui, and M. Benouis, ‘An Improved Behavioral Biometric System based on Gait and ECG signals’, *International Journal of Intelligent Engineering and Systems*, vol. 12, no. 6, pp. 147–156, 2019, doi: 10.22266/IJIES2019.1231.14.
- [3] A. Turner and S. Hayes, ‘The Classification of Minor Gait Alterations Using Wearable Sensors and Deep Learning’, *IEEE Trans Biomed Eng*, vol. 66, no. 11, pp. 3136–3145, Nov. 2019, doi: 10.1109/TBME.2019.2900863.
- [4] A. S. Alharthi, A. J. Casson, and K. B. Ozanyan, ‘Gait Spatiotemporal Signal Analysis for Parkinson’s Disease Detection and Severity Rating’, *IEEE Sens J*, vol. 21, no. 2, pp. 1838–1848, Jan. 2021, doi: 10.1109/JSEN.2020.3018262.
- [5] Y. Jeon, J. Kang, B. C. Kim, K. H. Lee, J. I. Song, and J. Gwak, ‘Early Alzheimer’s Disease Diagnosis Using Wearable Sensors and Multilevel Gait Assessment: A Machine Learning Ensemble Approach’, *IEEE Sens J*, vol. 23, no. 9, pp. 10041–10053, May 2023, doi: 10.1109/JSEN.2023.3259034.
- [6] L. Borzi, I. Mazzetta, A. Zampogna, A. Suppa, G. Olmo, and F. Irrera, ‘Prediction of freezing of gait in parkinson’s disease using wearables and machine learning’, *Sensors (Switzerland)*, vol. 21, no. 2, pp. 1–19, Jan. 2021, doi: 10.3390/s21020614.
- [7] R. Kaur, J. Levy, R. W. Motl, R. Sowers, and M. E. Hernandez, ‘Deep Learning for Multiple Sclerosis Differentiation Using Multi-Stride Dynamics in Gait’, *IEEE Trans Biomed Eng*, vol. 70, no. 7, pp. 2181–2192, Jul. 2023, doi: 10.1109/TBME.2023.3238680.
- [8] J. Kondragunta and G. Hirtz, ‘Gait Parameter Estimation of Elderly People using 3D Human Pose Estimation in Early Detection of Dementia’, in *2020 42nd Annual International Conference of the IEEE Engineering in Medicine & Biology Society (EMBC)*, IEEE, Jul. 2020, pp. 5798–5801. doi: 10.1109/EMBC44109.2020.9175766.
- [9] L. Donisi *et al.*, ‘Positive impact of short-term gait rehabilitation in Parkinson patients: A combined approach based on statistics and machine learning’,

- Mathematical Biosciences and Engineering*, vol. 18, no. 5, pp. 6995–7009, 2021, doi: 10.3934/MBE.2021348.
- [10] S. B. Richmond, C. W. Swanson, D. S. Peterson, and B. W. Fling, ‘A temporal analysis of bilateral gait coordination in people with multiple sclerosis’, *Mult Scler Relat Disord*, vol. 45, Oct. 2020, doi: 10.1016/j.msard.2020.102445.
- [11] W. Xiang, S. Yang, G. P. Adam, H. Zhang, W. Zuo, and J. Wen, ‘DC Fault Protection Algorithms of MMC-HVDC Grids: Fault Analysis, Methodologies, Experimental Validations, and Future Trends’, *IEEE Trans Power Electron*, vol. 36, no. 10, pp. 11245–11264, Oct. 2021, doi: 10.1109/TPEL.2021.3071184.
- [12] J. Aliasgari, M. Forouzandeh, and N. Karmakar, ‘Chipless RFID Readers for Frequency-Coded Tags: Time-Domain or Frequency-Domain?’, *IEEE Journal of Radio Frequency Identification*, vol. 4, no. 2, pp. 146–158, Jun. 2020, doi: 10.1109/JRFID.2020.2982822.
- [13] G. IEEE Engineering in Medicine and Biology Society. Annual International Conference (41st : 2019 : Berlin, IEEE Engineering in Medicine and Biology Society, and Institute of Electrical and Electronics Engineers, *2019 41st Annual International Conference of the IEEE Engineering in Medicine and Biology Society (EMBC) : Biomedical Engineering Ranging from Wellness to Intensive Care : 41st EMB Conference 2019 : July 23-27, Berlin*.
- [14] Y. Zhang and Y. Ma, ‘Application of supervised machine learning algorithms in the classification of sagittal gait patterns of cerebral palsy children with spastic diplegia’, *Comput Biol Med*, vol. 106, pp. 33–39, Mar. 2019, doi: 10.1016/j.combiomed.2019.01.009.
- [15] M. Sarshar, S. Polturi, and L. Schega, ‘Gait phase estimation by using lstm in imu-based gait analysis—proof of concept’, *Sensors*, vol. 21, no. 17, Sep. 2021, doi: 10.3390/s21175749.
- [16] D. Jarchi, J. Pope, T. K. M. Lee, L. Tamjidi, A. Mirzaei, and S. Sanei, ‘A Review on Accelerometry-Based Gait Analysis and Emerging Clinical Applications’, *IEEE Reviews in Biomedical Engineering*, vol. 11. Institute of Electrical and Electronics Engineers, pp. 177–194, Feb. 15, 2018. doi: 10.1109/RBME.2018.2807182.
- [17] M. Kumar, N. Singh, R. Kumar, S. Goel, and K. Kumar, ‘Gait recognition based on vision systems: A systematic survey’, *J Vis Commun Image Represent*, vol. 75, Feb. 2021, doi: 10.1016/j.jvcir.2021.103052.

- [18] G. Ciciirelli, D. Impedovo, V. Dentamaro, R. Marani, G. Pirlo, and T. R. D’Orazio, ‘Human Gait Analysis in Neurodegenerative Diseases: A Review’, *IEEE J Biomed Health Inform*, vol. 26, no. 1, pp. 229–242, Jan. 2022, doi: 10.1109/JBHI.2021.3092875.
- [19] IEEE Engineering in Medicine and Biology Society. Annual International Conference (42nd : 2020 : Online), IEEE Engineering in Medicine and Biology Society, Institute of Electrical and Electronics Engineers, and Canadian Medical and Biological Engineering Society. Annual Conference (43rd : 2020 : Online), *42nd Annual International Conferences of the IEEE Engineering in Medicine and Biology Society : ‘Enabling Innovative Technologies for Global Healthcare’ : 20-24 July 2020, Montreal, Canada*.
- [20] L. Ruiz-Ruiz, A. R. Jimenez, G. Garcia-Villamil, and F. Seco, ‘Detecting fall risk and frailty in elders with inertial motion sensors: A survey of significant gait parameters’, *Sensors*, vol. 21, no. 20. MDPI, Oct. 01, 2021. doi: 10.3390/s21206918.
- [21] A. G. Moraes *et al.*, ‘Effect of hippotherapy on walking performance and gait parameters in people with multiple sclerosis’, *Mult Scler Relat Disord*, vol. 43, Aug. 2020, doi: 10.1016/j.msard.2020.102203.
- [22] N. F. Ribeiro and C. P. Santos, ‘Inertial measurement units: A brief state of the art on gait analysis’, in *ENBENG 2017 - 5th Portuguese Meeting on Bioengineering, Proceedings*, Institute of Electrical and Electronics Engineers Inc., Mar. 2017. doi: 10.1109/ENBENG.2017.7889458.
- [23] E. P. Washabaugh, T. Kalyanaraman, P. G. Adamczyk, E. S. Claffin, and C. Krishnan, ‘Validity and repeatability of inertial measurement units for measuring gait parameters’, *Gait Posture*, vol. 55, pp. 87–93, Jun. 2017, doi: 10.1016/j.gaitpost.2017.04.013.
- [24] M. Paulich, M. Schepers, N. Rudigkeit, and G. Bellusci, ‘Xsens MTw Awinda: Miniature Wireless Inertial-Magnetic Motion Tracker for Highly Accurate 3D Kinematic Applications’. [Online]. Available: www.xsens.com,
- [25] K. Trentzsch *et al.*, ‘Using machine learning algorithms for identifying gait parameters suitable to evaluate subtle changes in gait in people with multiple sclerosis’, *Brain Sci*, vol. 11, no. 8, Aug. 2021, doi: 10.3390/brainsci11081049.

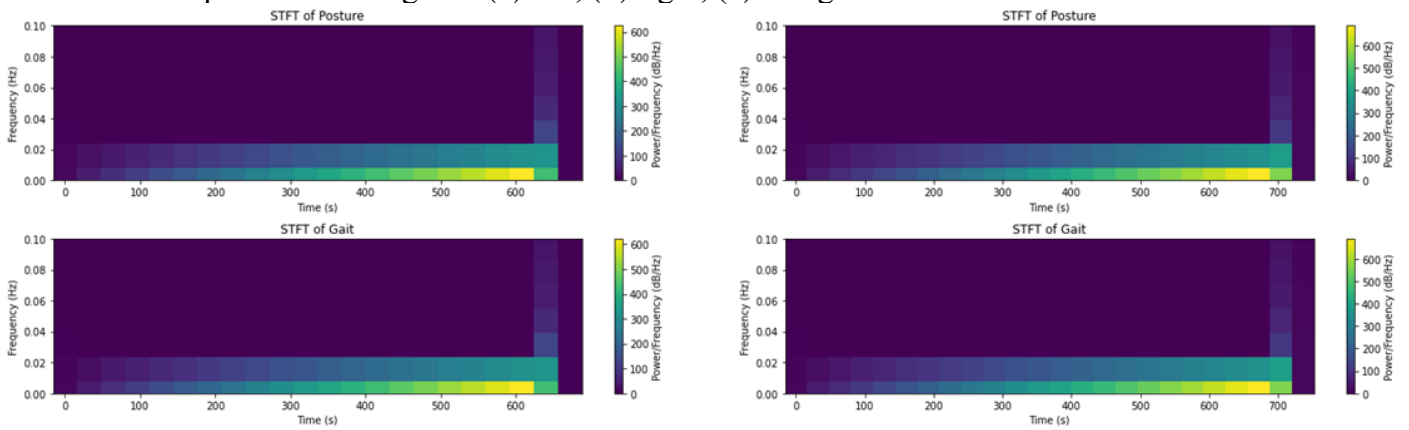
- [26] G. Rescio, A. Leone, and P. Siciliano, ‘Supervised machine learning scheme for electromyography-based pre-fall detection system’, *Expert Syst Appl*, vol. 100, pp. 95–105, Jun. 2018, doi: 10.1016/j.eswa.2018.01.047.
- [27] C. Morbidoni, A. Cucchiarelli, S. Fioretti, and F. Di Nardo, ‘A deep learning approach to EMG-based classification of gait phases during level ground walking’, *Electronics (Switzerland)*, vol. 8, no. 8, Aug. 2019, doi: 10.3390/electronics8080894.
- [28] K. Jun, S. Lee, D. W. Lee, and M. S. Kim, ‘Deep Learning-Based Multimodal Abnormal Gait Classification Using a 3D Skeleton and Plantar Foot Pressure’, *IEEE Access*, vol. 9, pp. 161576–161589, 2021, doi: 10.1109/ACCESS.2021.3131613.
- [29] S. S. Lee, S. T. Choi, and S. Il Choi, ‘Classification of gait type based on deep learning using various sensors with smart insole’, *Sensors (Switzerland)*, vol. 19, no. 8, Apr. 2019, doi: 10.3390/s19081757.
- [30] G. IEEE Engineering in Medicine and Biology Society. Annual International Conference (41st : 2019 : Berlin, IEEE Engineering in Medicine and Biology Society, and Institute of Electrical and Electronics Engineers, *2019 41st Annual International Conference of the IEEE Engineering in Medicine and Biology Society (EMBC) : Biomedical Engineering Ranging from Wellness to Intensive Care : 41st EMB Conference 2019 : July 23-27, Berlin*.
- [31] Y. Jing *et al.*, ‘Deep Learning–Assisted Gait Parameter Assessment for Neurodegenerative Diseases: Model Development and Validation’, *J Med Internet Res*, vol. 25, p. e46427, Jul. 2023, doi: 10.2196/46427.
- [32] Z. Li, F. Liu, W. Yang, S. Peng, and J. Zhou, ‘A Survey of Convolutional Neural Networks: Analysis, Applications, and Prospects’, *IEEE Trans Neural Netw Learn Syst*, vol. 33, no. 12, pp. 6999–7019, Dec. 2022, doi: 10.1109/TNNLS.2021.3084827.
- [33] M. Krichen, ‘Convolutional Neural Networks: A Survey’, *Computers*, vol. 12, no. 8, Aug. 2023, doi: 10.3390/computers12080151.
- [34] Y. Tian, ‘Artificial Intelligence Image Recognition Method Based on Convolutional Neural Network Algorithm’, *IEEE Access*, vol. 8, pp. 125731–125744, 2020, doi: 10.1109/ACCESS.2020.3006097.
- [35] S. K. Paramasivan, ‘Deep learning based recurrent neural networks to enhance the performance of wind energy forecasting: A review’, *Revue d’Intelligence*

- Artificielle*, vol. 35, no. 1. International Information and Engineering Technology Association, pp. 1–10, Feb. 01, 2021. doi: 10.18280/ria.350101.
- [36] J. Zhang, H. Liu, Q. Chang, L. Wang, and R. X. Gao, ‘Recurrent neural network for motion trajectory prediction in human-robot collaborative assembly’, *CIRP Annals*, vol. 69, no. 1, pp. 9–12, Jan. 2020, doi: 10.1016/j.cirp.2020.04.077.
- [37] M. O. Oloyede and G. P. Hancke, ‘Unimodal and Multimodal Biometric Sensing Systems: A Review’, *IEEE Access*, vol. 4. Institute of Electrical and Electronics Engineers Inc., pp. 7532–7555, 2016. doi: 10.1109/ACCESS.2016.2614720.
- [38] P. Jangid, G. Nilesh Sawant, V. Ashok Bharadi, and N. Giri, ‘International Journal of INTELLIGENT SYSTEMS AND APPLICATIONS IN ENGINEERING Performance Analysis of Deep Neural Networks for Unimodal and Multimodal Biometric Authentication’. [Online]. Available: www.ijisae.org
- [39] A. Mikołajczyk and M. Grochowski, ‘Data augmentation for improving deep learning in image classification problem’, in *2018 International Interdisciplinary PhD Workshop, IIPhDW 2018*, Institute of Electrical and Electronics Engineers Inc., Jun. 2018, pp. 117–122. doi: 10.1109/IIPHDW.2018.8388338.
- [40] A. S. B. Azam, A. K. Jumaat, and S. Ibrahim, ‘Comparison of Various Colorization Techniques for MRI Brain Tumor Segmentation using Convolutional Neural Networks’, in *8th International Conference on Recent Advances and Innovations in Engineering: Empowering Computing, Analytics, and Engineering Through Digital Innovation, ICRAIE 2023*, Institute of Electrical and Electronics Engineers Inc., 2023. doi: 10.1109/ICRAIE59459.2023.10468529.
- [41] Y. Bai *et al.*, ‘Understanding and Improving Early Stopping for Learning with Noisy Labels’. [Online]. Available: <https://github.com/tmllab/PES>.

APPENDICES

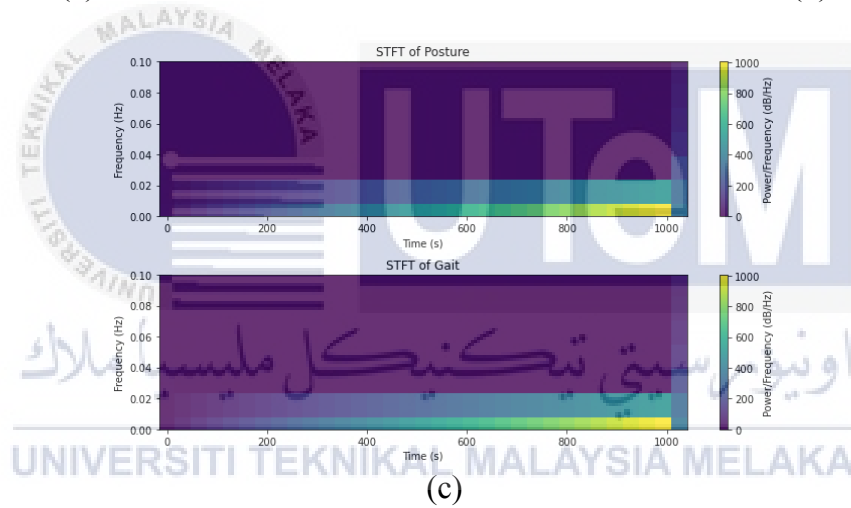
APPENDIX A TFR OF PARTICIPANTS

Participant 2 TFR diagram. (a) left, (b) right, (c) straight.



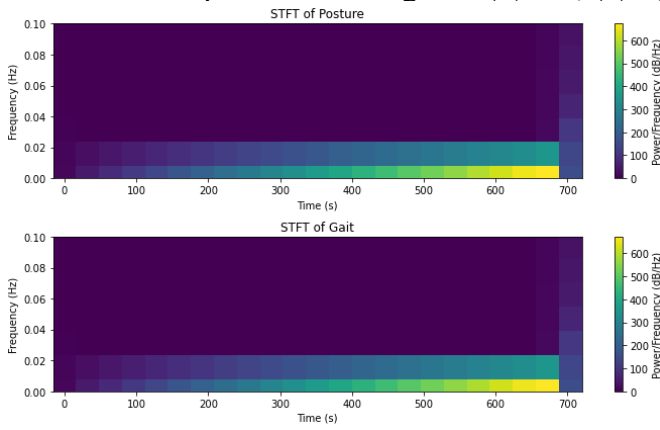
(a)

(b)

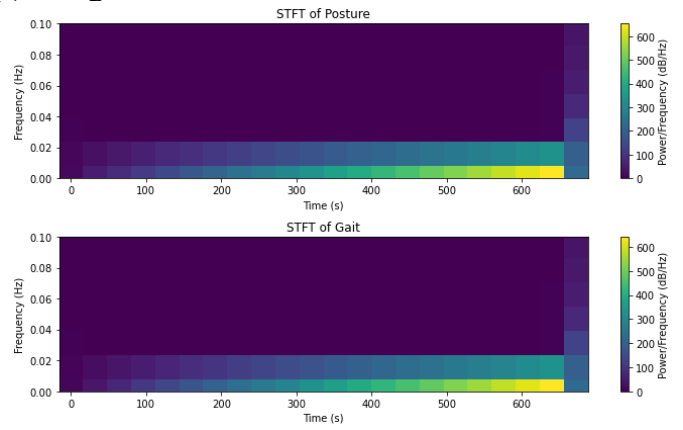


(c)

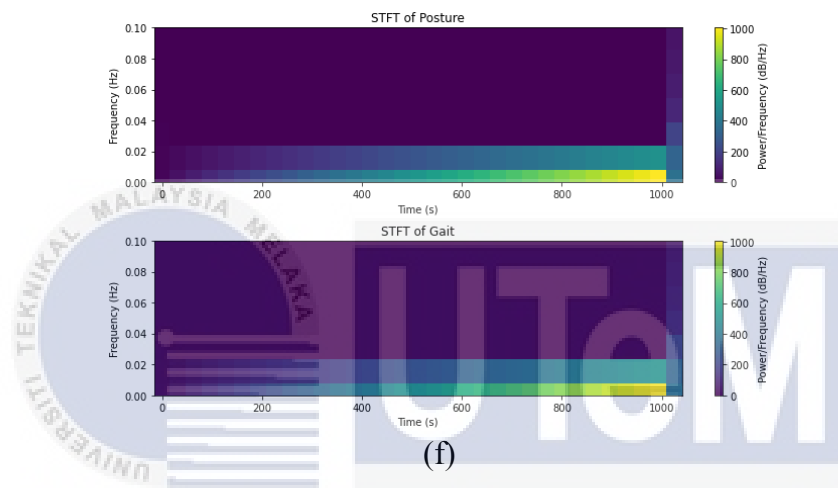
Participant 3 TFR diagram. (d) left, (e) right, (f) straight.



(d)



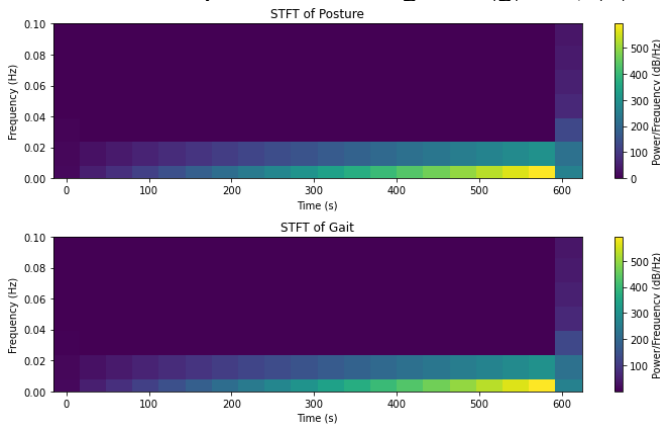
(e)



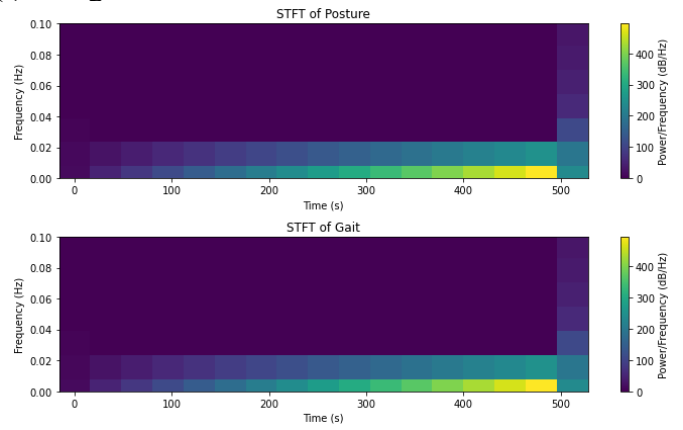
(f)

اونيورسيتي تيكنيكل مليسيا ملاك
UNIVERSITI TEKNIKAL MALAYSIA MELAKA

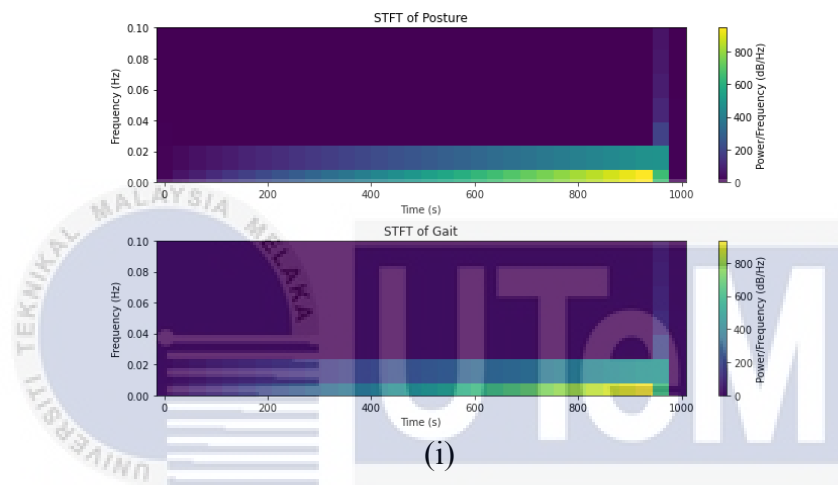
Participant 4 TFR diagram. (g) left, (h) right, (i) straight.



(g)



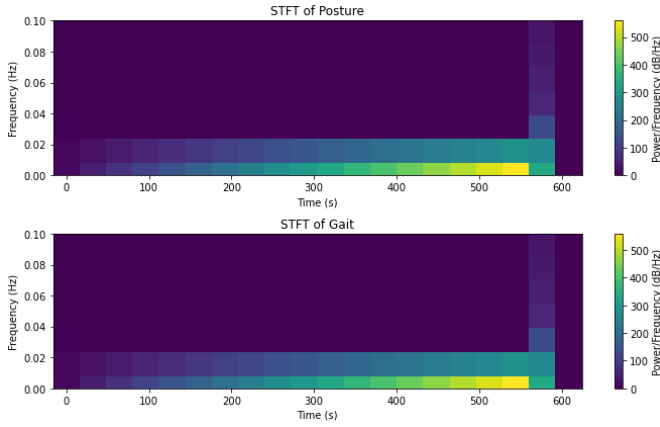
(h)



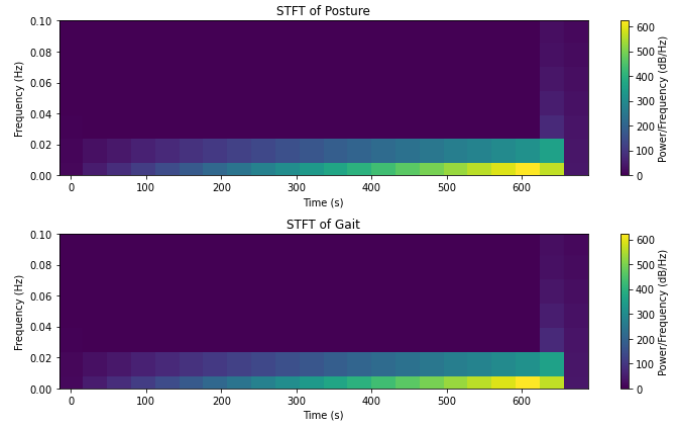
(i)

اونيورسيتي تيكنيكل مليسيا ملاك
UNIVERSITI TEKNIKAL MALAYSIA MELAKA

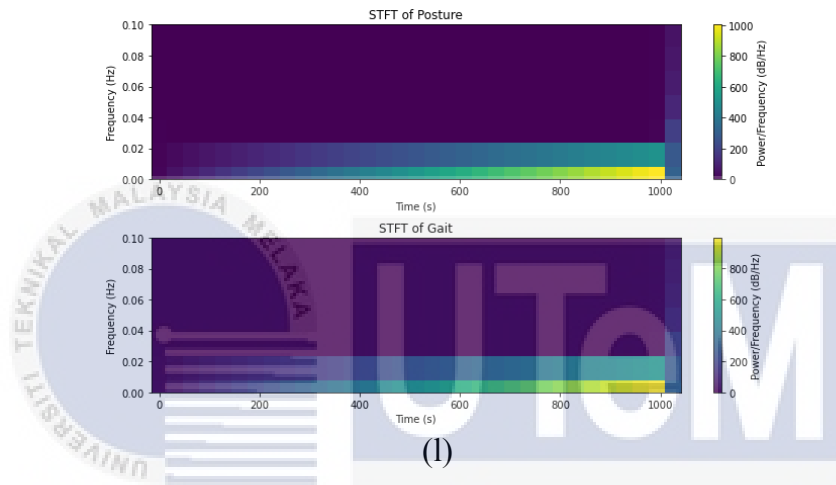
Participant 5 TFR diagram. (j) left, (k) right, (l) straight.



(j)



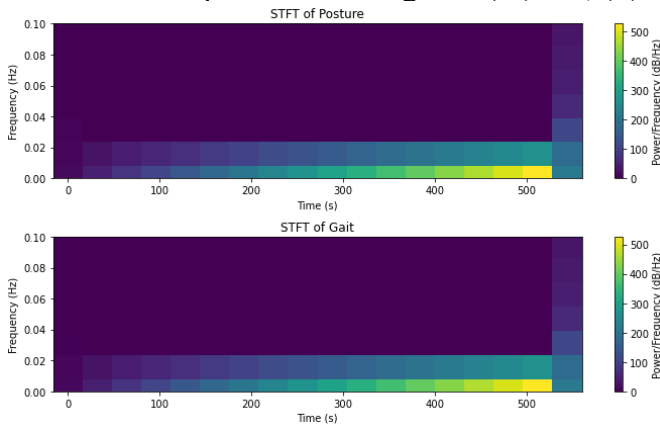
(k)



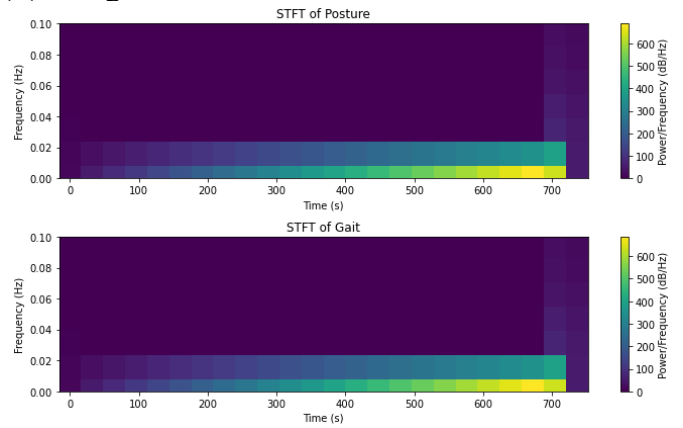
(l)

اونيورسيتي تيكنيكل مليسيا ملاك
UNIVERSITI TEKNIKAL MALAYSIA MELAKA

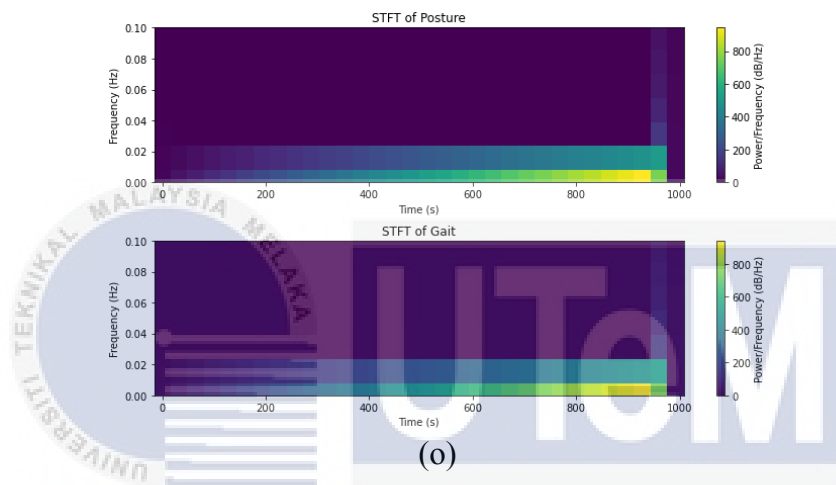
Participant 6 TFR diagram. (m) left, (n) right, (o) straight.



(m)



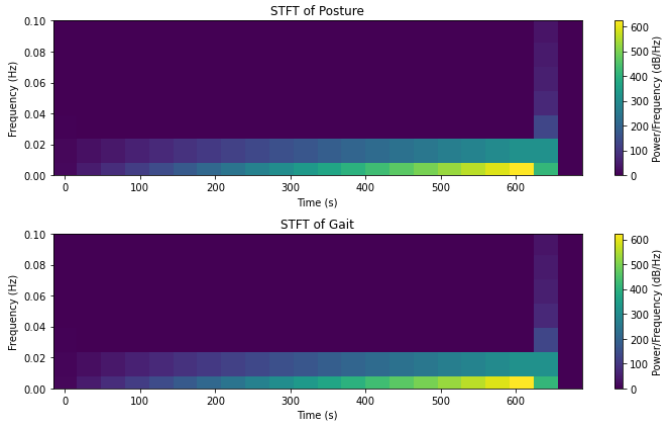
(n)



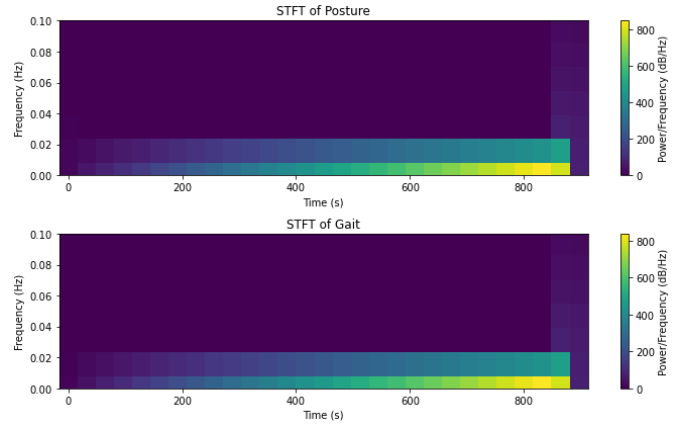
(o)

اونيورسيتي تيكنيكل مليسيا ملاك
UNIVERSITI TEKNIKAL MALAYSIA MELAKA

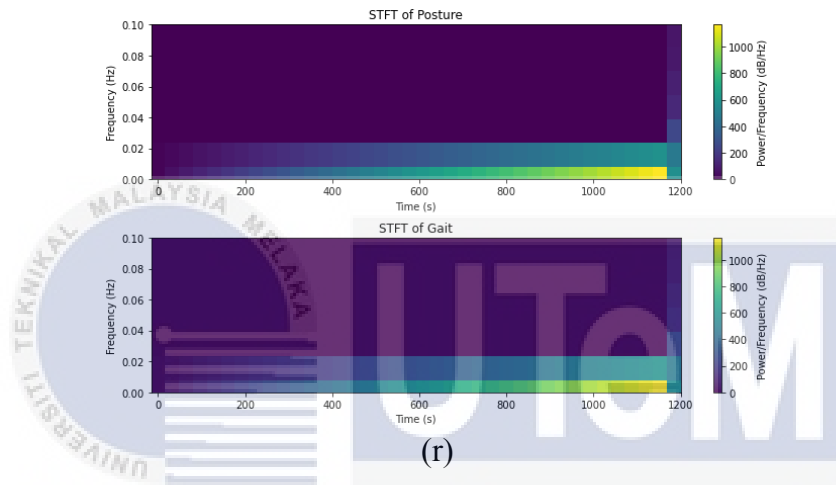
Participant 7 TFR diagram. (p) left, (q) right, (r) straight.



(p)



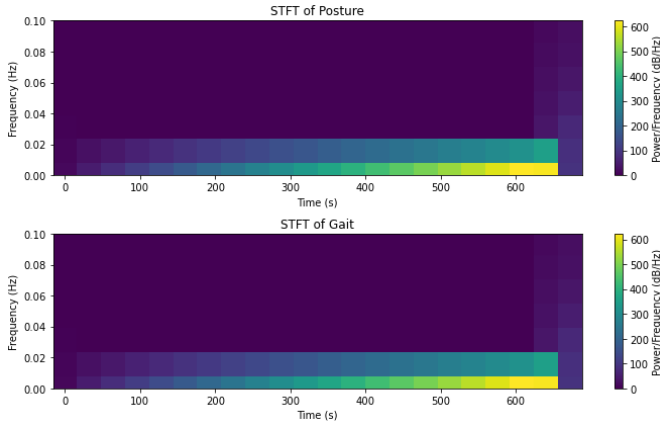
(q)



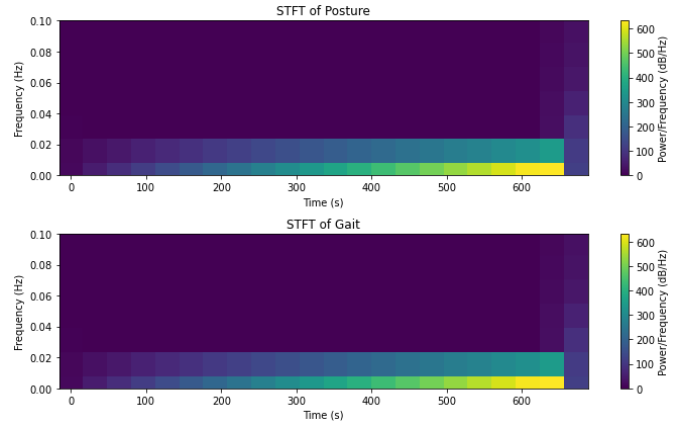
(r)

اونيورسيتي تيكنيكل مليسيا ملاك
UNIVERSITI TEKNIKAL MALAYSIA MELAKA

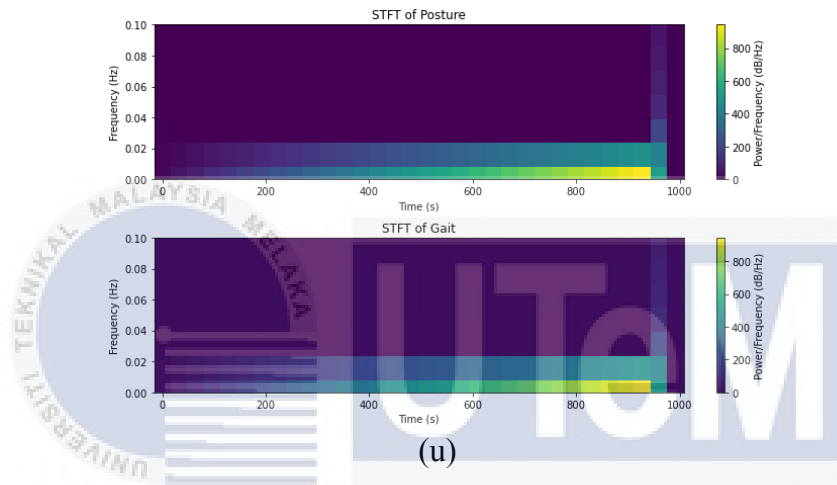
Participant 8 TFR diagram. (s) left, (t) right, (u) straight.



(s)



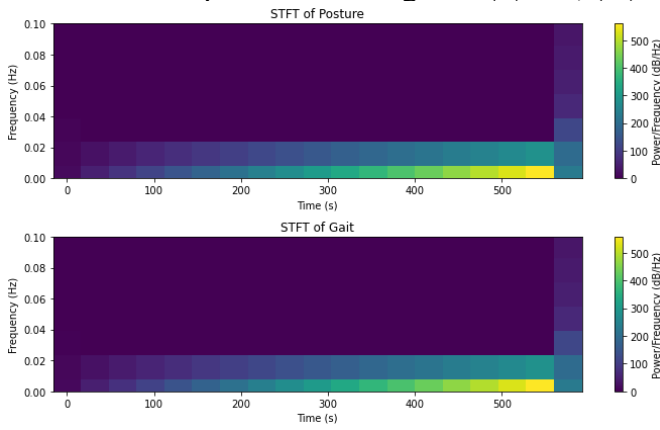
(t)



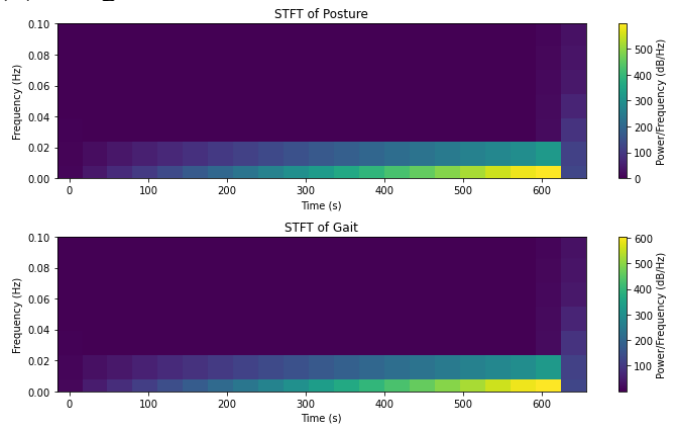
(u)

اونيورسيتي تيكنيكل مليسيا ملاك
UNIVERSITI TEKNIKAL MALAYSIA MELAKA

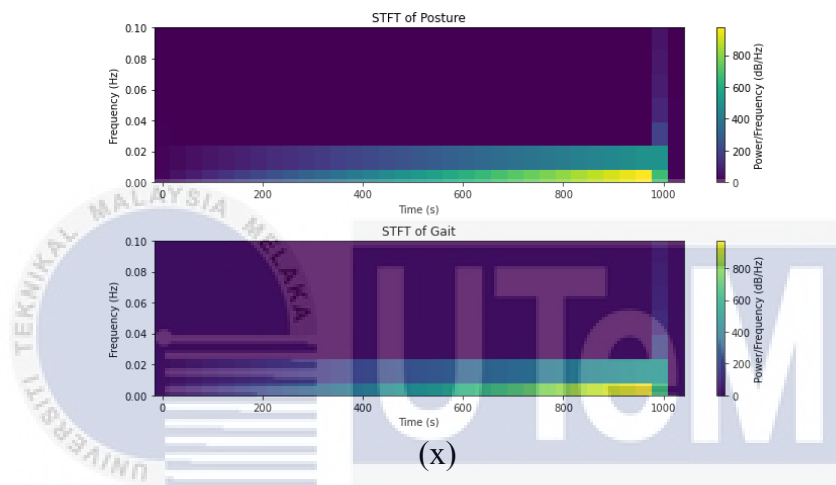
Participant 9 TFR diagram. (v) left, (w) right, (x) straight.



(v)



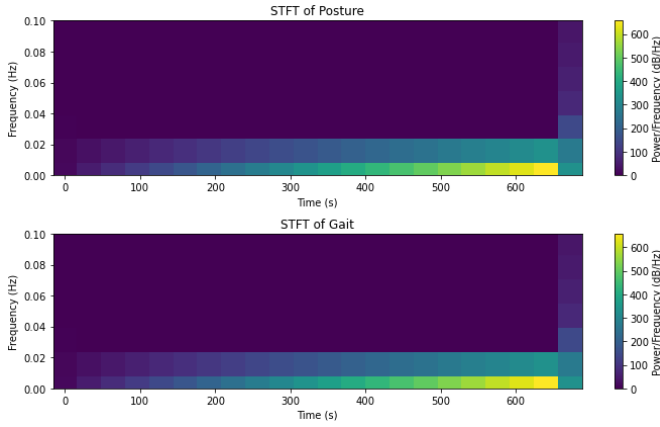
(w)



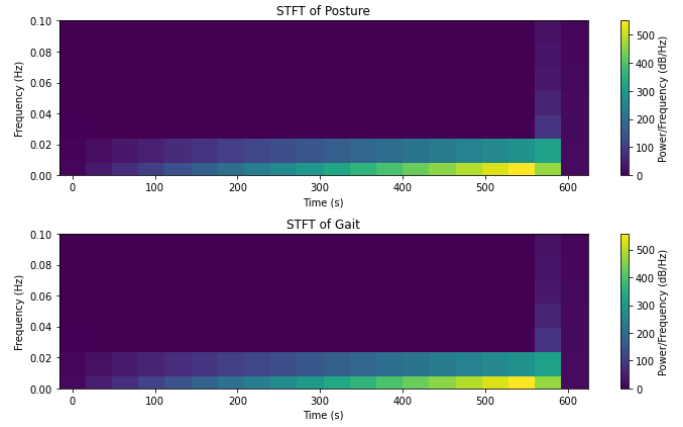
(x)

اونيورسيتي تيكنيكل مليسيا ملاك
UNIVERSITI TEKNIKAL MALAYSIA MELAKA

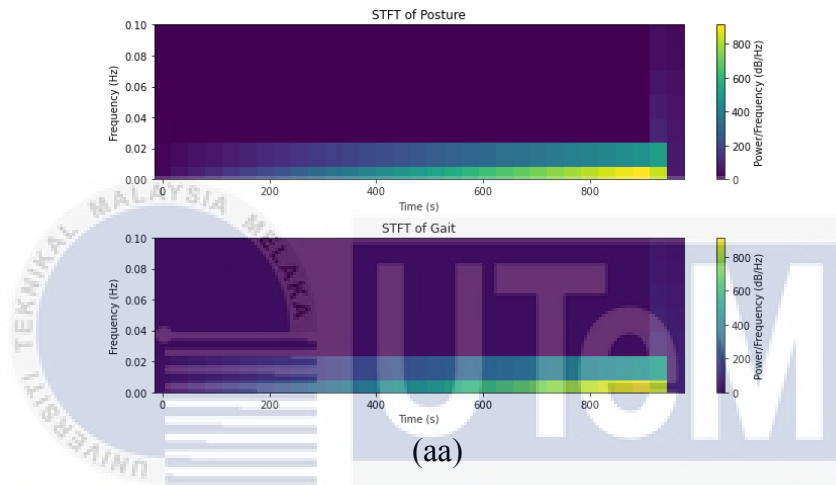
Participant 10 TFR diagram. (y) left, (z) right, (aa) straight.



(y)



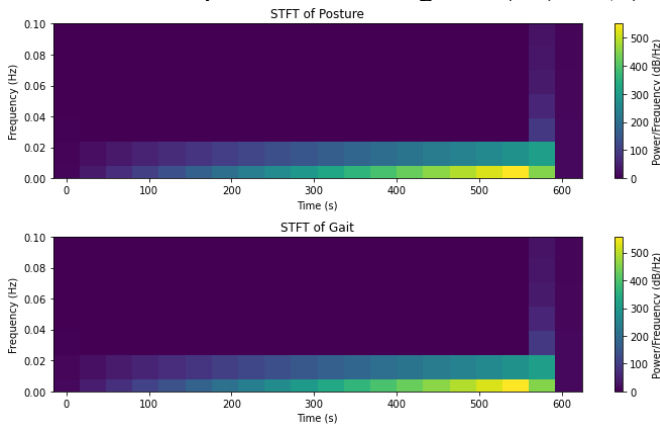
(z)



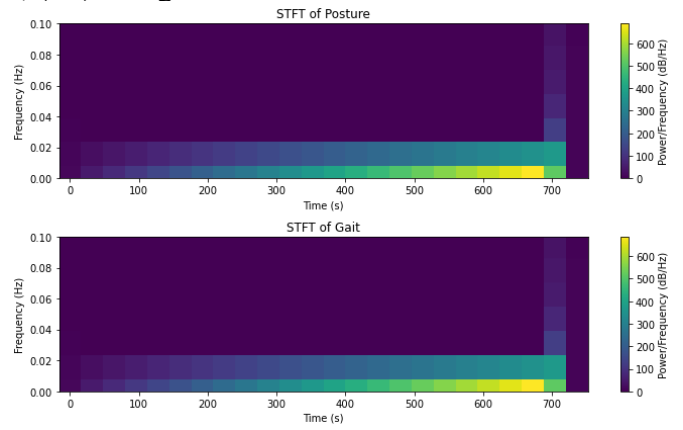
(aa)

اونيورسيتي تيكنيكل مليسيا ملاك
UNIVERSITI TEKNIKAL MALAYSIA MELAKA

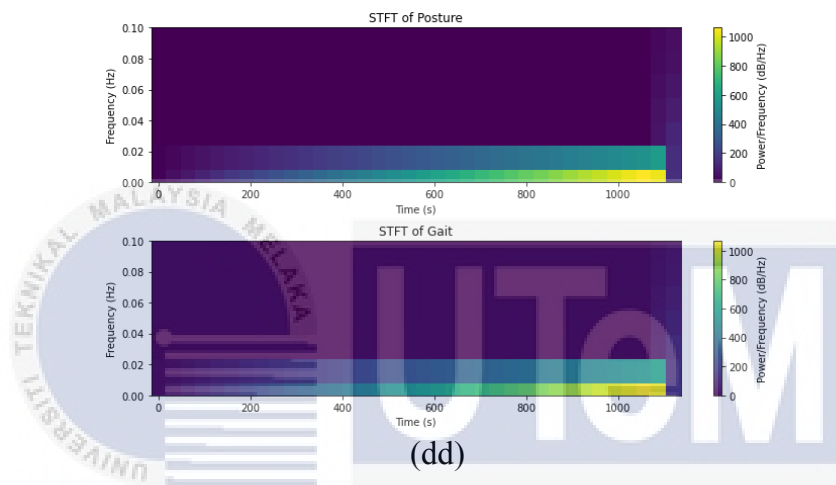
Participant 11 TFR diagram. (bb) left, (cc) right, (dd) straight.



(bb)



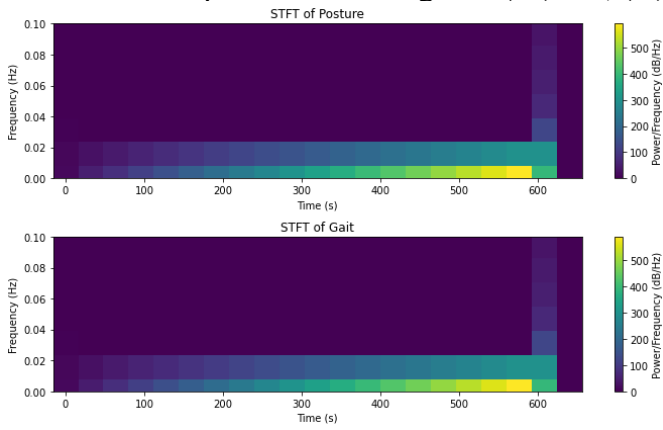
(cc)



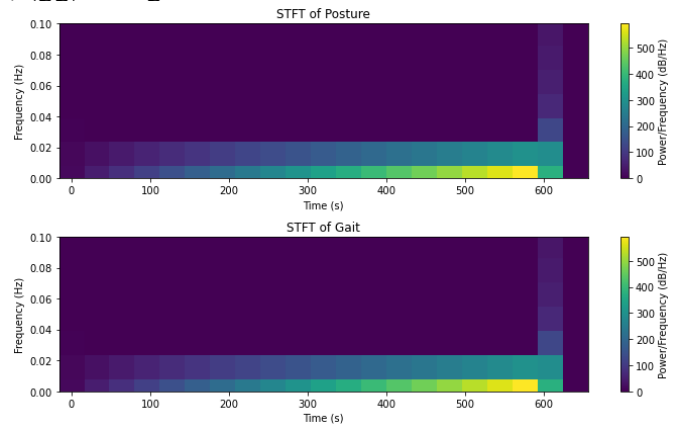
(dd)

اونيورسيتي تيكنيكل مليسيا ملاك
UNIVERSITI TEKNIKAL MALAYSIA MELAKA

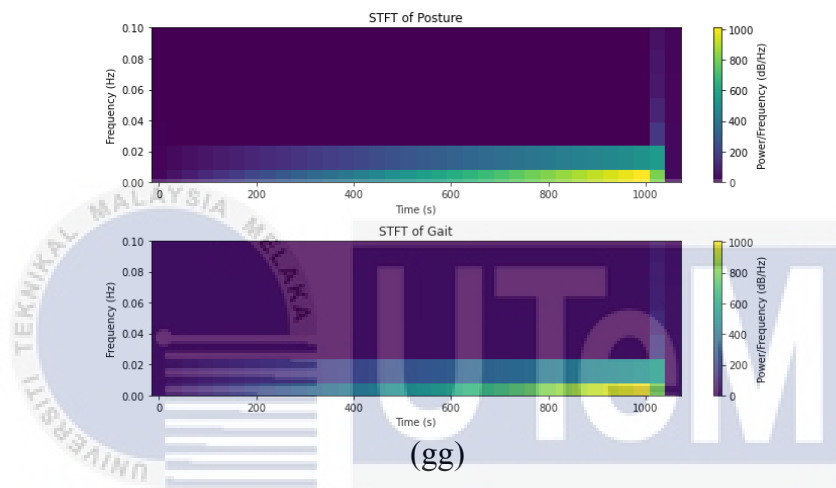
Participant 12 TFR diagram. (ee) left, (ff) right, (gg) straight.



(ee)

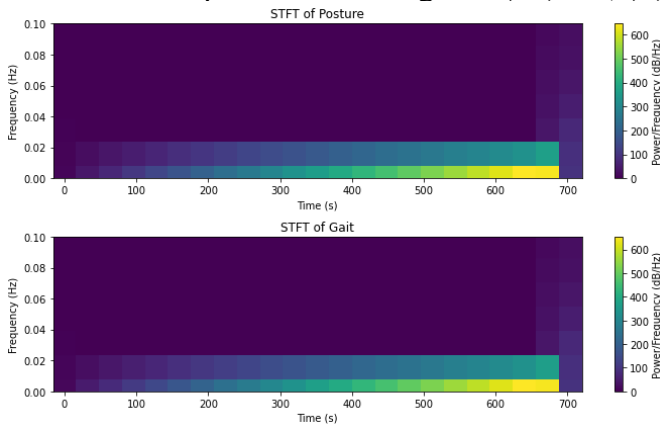


(ff)

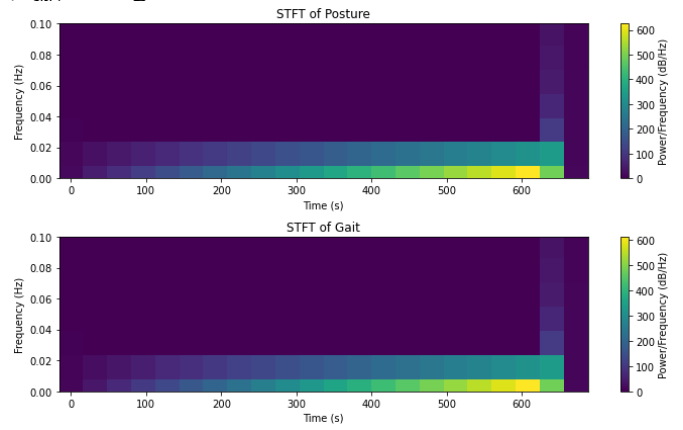


(gg)

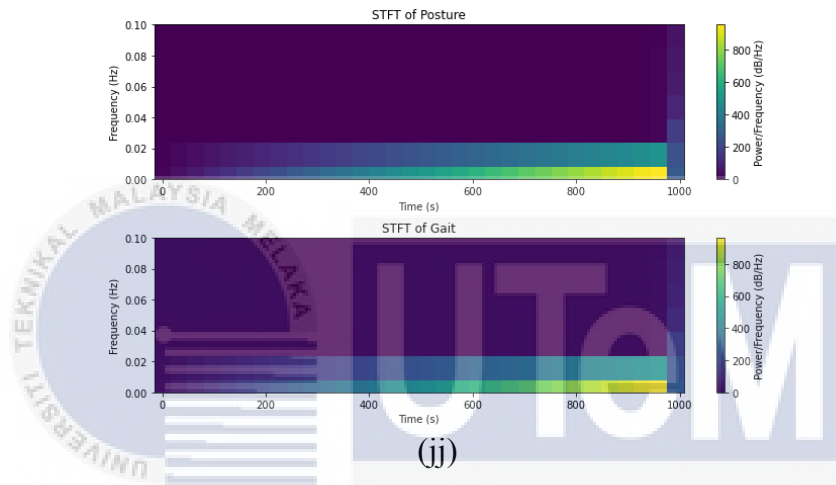
Participant 13 TFR diagram. (hh) left, (ii) right, (jj) straight.



(hh)



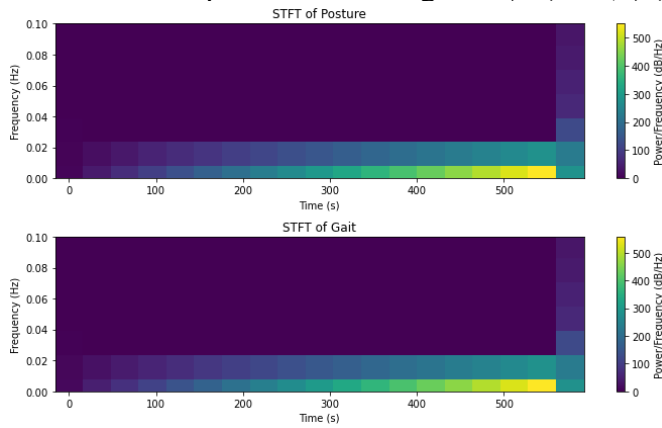
(ii)



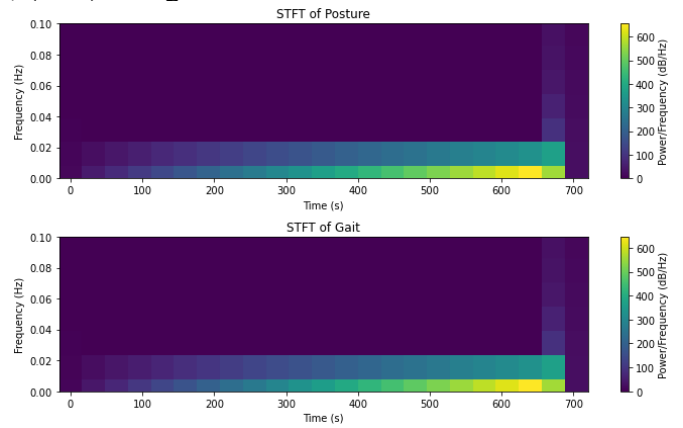
(jj)

اونيورسيتي تيكنيكل مليسيا ملاك
UNIVERSITI TEKNIKAL MALAYSIA MELAKA

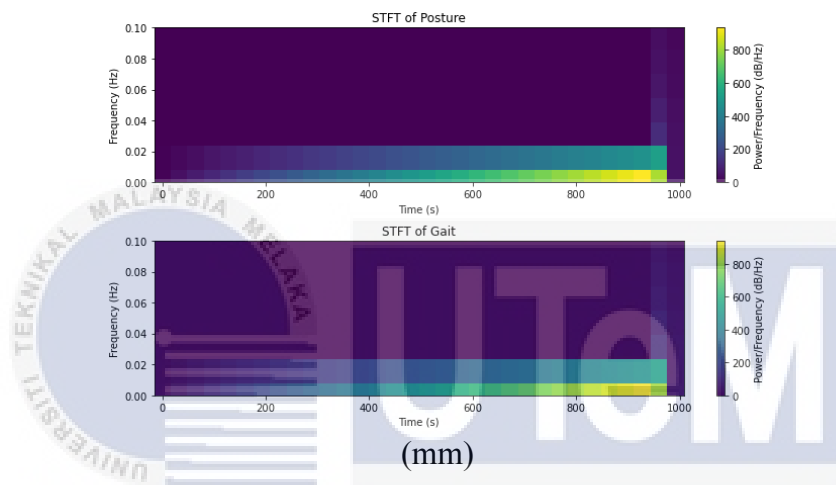
Participant 14 TFR diagram. (kk) left, (ll) right, (mm) straight.



(kk)



(ll)



(mm)

اونيورسيتي تيكنيكل مليسيا ملاك
UNIVERSITI TEKNIKAL MALAYSIA MELAKA

APPENDIX B PARTICIPANTS METADATA

| Participant ID | Gender | Age (years) | Body mass (kg) | Body height (m) | Hip height (m) | Shoe Lenght | Shoulder Height | Shoulder Width | Elbow Span | Wrist Span | Arm Span | Hip Width | Knee Height | Ankle Height |
|----------------|--------|-------------|----------------|-----------------|----------------|-------------|-----------------|----------------|------------|------------|----------|-----------|-------------|--------------|
| participant01 | M | 23 | 63 | 1.8 | 1.02 | 0.3 | 1.52 | 0.31 | 0.86 | 1.38 | 1.74 | 0.27 | 0.53 | 0.1 |
| participant02 | F | 24 | 50.5 | 1.51 | 0.86 | 0.25 | 1.18 | 0.25 | 0.77 | 1.18 | 1.51 | 0.25 | 0.45 | 0.08 |
| participant03 | M | 22 | 89 | 1.85 | 1.07 | 0.3 | 1.54 | 0.39 | 1.06 | 1.51 | 1.88 | 0.3 | 0.53 | 0.11 |
| participant04 | F | 28 | 70 | 1.59 | 0.95 | 0.27 | 1.36 | 0.36 | 0.83 | 1.27 | 1.56 | 0.32 | 0.49 | 0.1 |
| participant05 | F | 27 | 53 | 1.57 | 0.91 | 0.26 | 1.3 | 0.31 | 0.81 | 1.28 | 1.59 | 0.29 | 0.43 | 0.09 |
| participant06 | M | 30 | 68 | 1.72 | 0.95 | 0.28 | 1.4 | 0.28 | 0.86 | 1.38 | 1.78 | 0.25 | 0.5 | 0.1 |
| participant07 | M | 28 | 75 | 1.85 | 1.01 | 0.29 | 1.48 | 0.32 | 0.97 | 1.47 | 1.87 | 0.31 | 0.53 | 0.1 |
| participant08 | M | 24 | 86 | 1.7 | 0.93 | 0.29 | 1.38 | 0.31 | 0.82 | 1.36 | 1.67 | 0.29 | 0.46 | 0.09 |
| participant09 | M | 24 | 72.7 | 1.7 | 0.92 | 0.28 | 1.36 | 0.31 | 0.92 | 1.34 | 1.72 | 0.28 | 0.43 | 0.11 |
| participant10 | M | 26 | 84 | 1.75 | 0.95 | 0.29 | 1.47 | 0.38 | 0.97 | 1.35 | 1.74 | 0.28 | 0.52 | 0.09 |
| participant11 | M | 23 | 64 | 1.72 | 0.94 | 0.27 | 1.42 | 0.32 | 0.9 | 1.35 | 1.73 | 0.24 | 0.49 | 0.1 |
| participant12 | M | 26 | 64 | 1.75 | 0.93 | 29 | 1.39 | 0.35 | 0.95 | 1.35 | 1.76 | 0.3 | 0.5 | 0.9 |
| participant13 | M | 26 | 74 | 1.82 | 1 | 0.29 | 1.47 | 0.28 | 0.97 | 1.47 | 1.85 | 0.25 | 0.52 | 0.1 |
| participant14 | F | 24 | 63 | 1.71 | 0.98 | 0.27 | 1.39 | 0.31 | 0.92 | 1.29 | 1.69 | 0.28 | 0.51 | 0.09 |

